# Volcanism in Eastern Oregon

Deep Mantle Plume?

Upper Mantle Plume?

Back-arc Basin?

Something Else?

# Three ways to melt the mantle

- Add water
- Add heat
- Reduce pressure

6 M Paulina Basalt flows Cove Palisades, Madras, Oregon

Cove Palisades Intra-Canyon Flow

Base of lower sequence, Cove Palisades

Smith Rocks State Park: ignimbrite flows & intrusive necks


John Day Formation in foreground, Rattlesnake Tuff on ridge

Picture Gorge Basalts, John Day River


Hart Mountain

West flank, Steens Mountain

# Faulted east flank, Steens Mountain

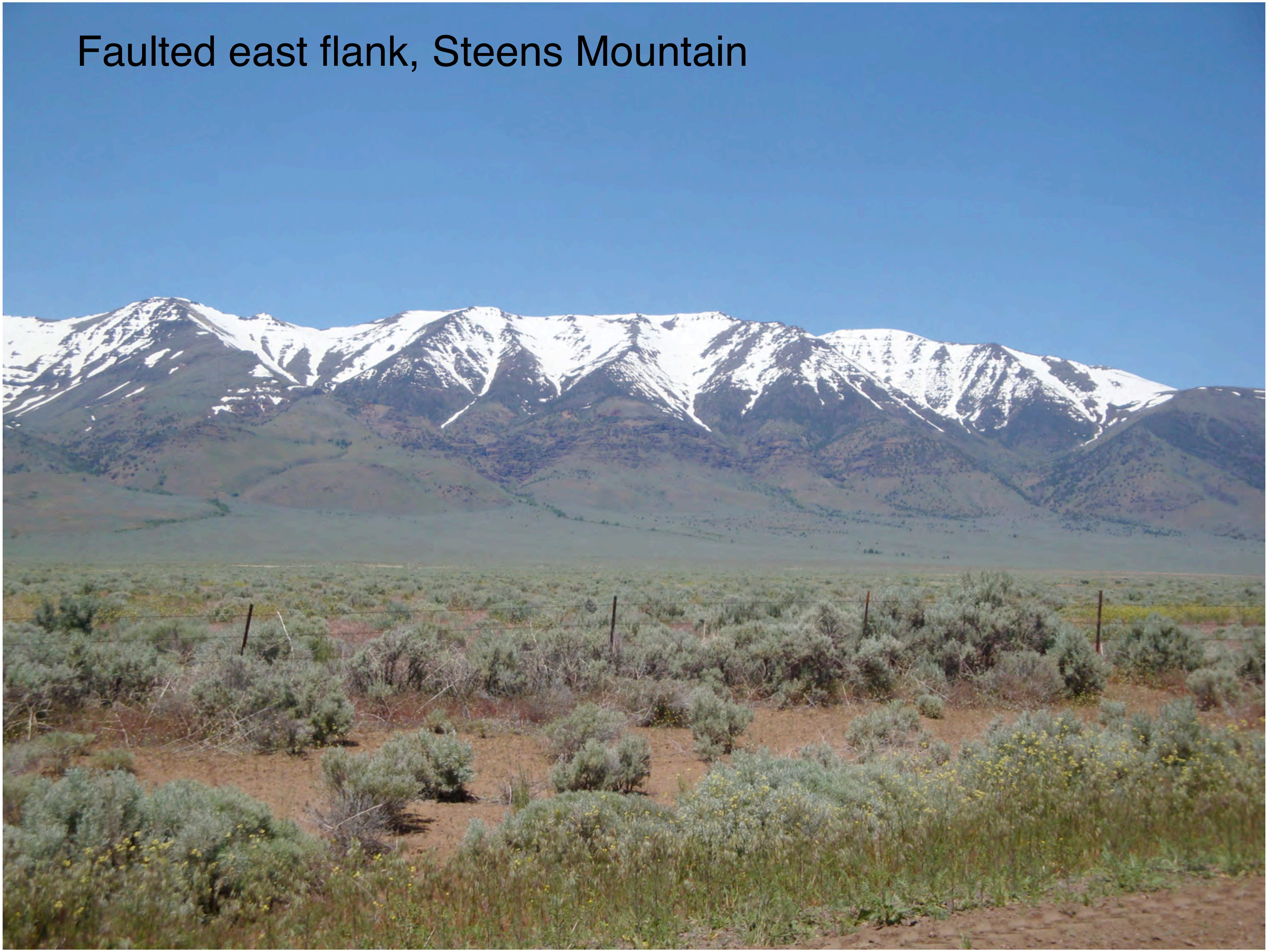

# Wildhorse Canyon, west flank, Steens Mountain

http://www.blm.gov/or/districts/burns/recreation/images/steens-kiger.jpg


Oregon-Idaho Graben, near Juntura, OR

I-84 between Ontario and Baker City

# Seven Devils Mountains above Hell's Canyon


CRB west side Hell's Canyon

CRB Dikes in Wallowa Granite


Wallula Gap, Columbia River


Geologists in field gear, CRB, Wallula Gap

Haystack Rock,Cannon Beach . . .

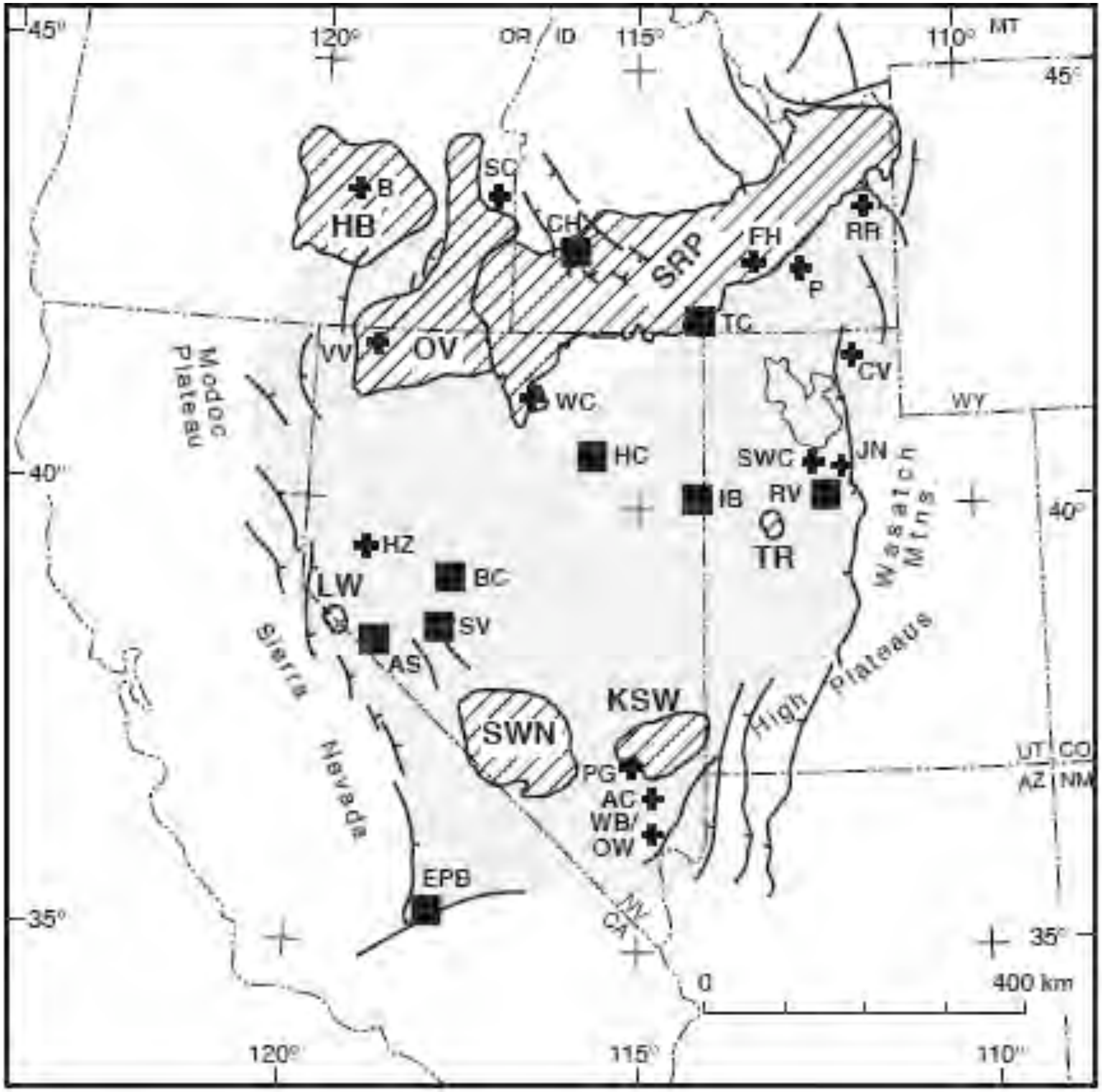


# Miocene Silicic Volcanic Centers

Streck and Ferns (2004)

# The Rattlesnake Tuff and other Miocene silicic volcanism in Eastern Oregon

Field Trip Guide
2004 GSA Cordilleran Meeting

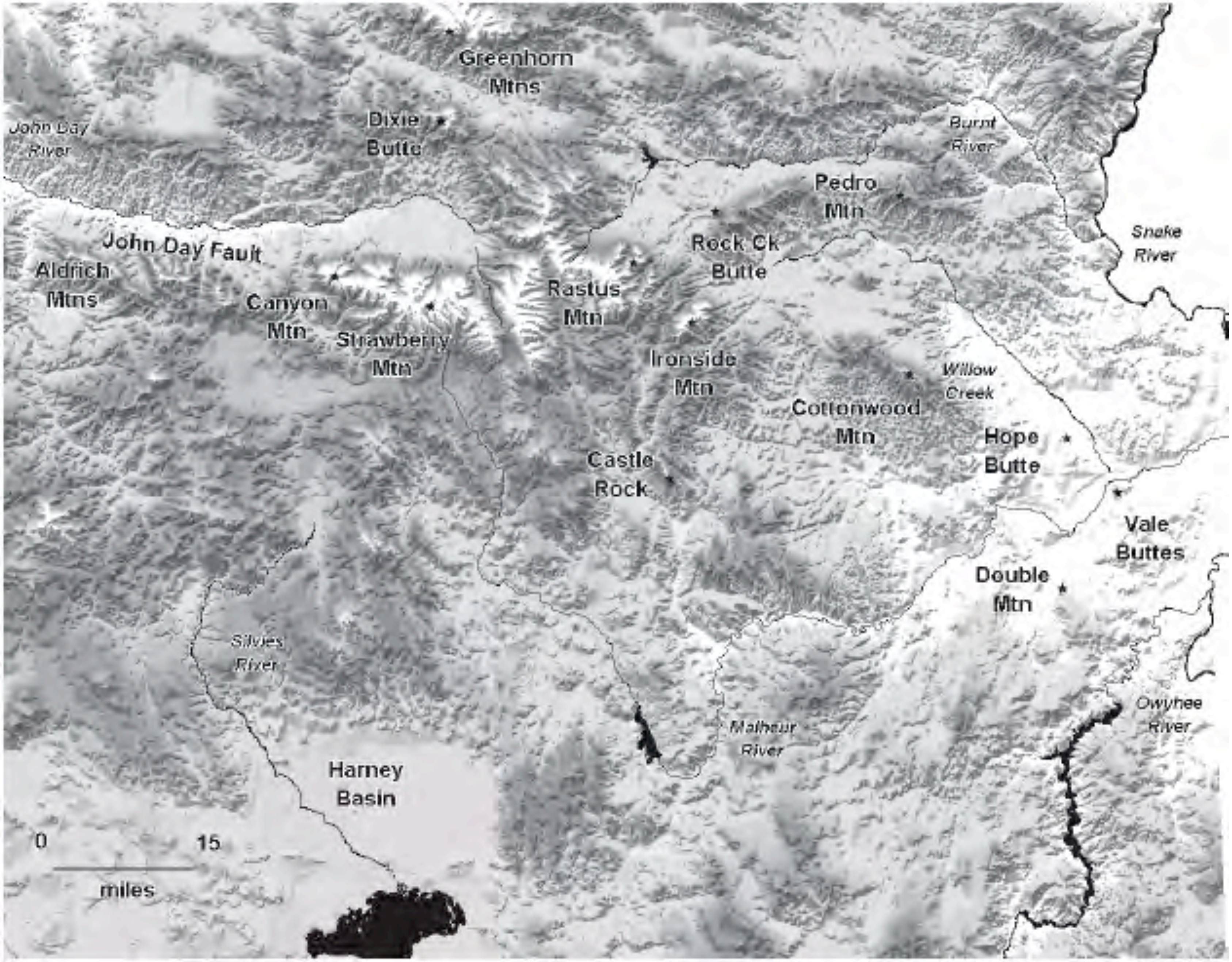
Greenhorn Mtns
Dixie Butte
John Day River
Burnt River
Pedro Mtn
Snake River
John Day Fault
Rock Ck Butte
Aldrich Mtns
Canyon Mtn
Rastus Mtn
Strawberry Mtn
Ironside Mtn
Willow Creek
Cottonwood Mtn
Hope Butte
Castle Rock
Vale Buttes
Double Mtn
Silvies River
Malheur River
Owyhee River
Harney Basin
0
15
miles

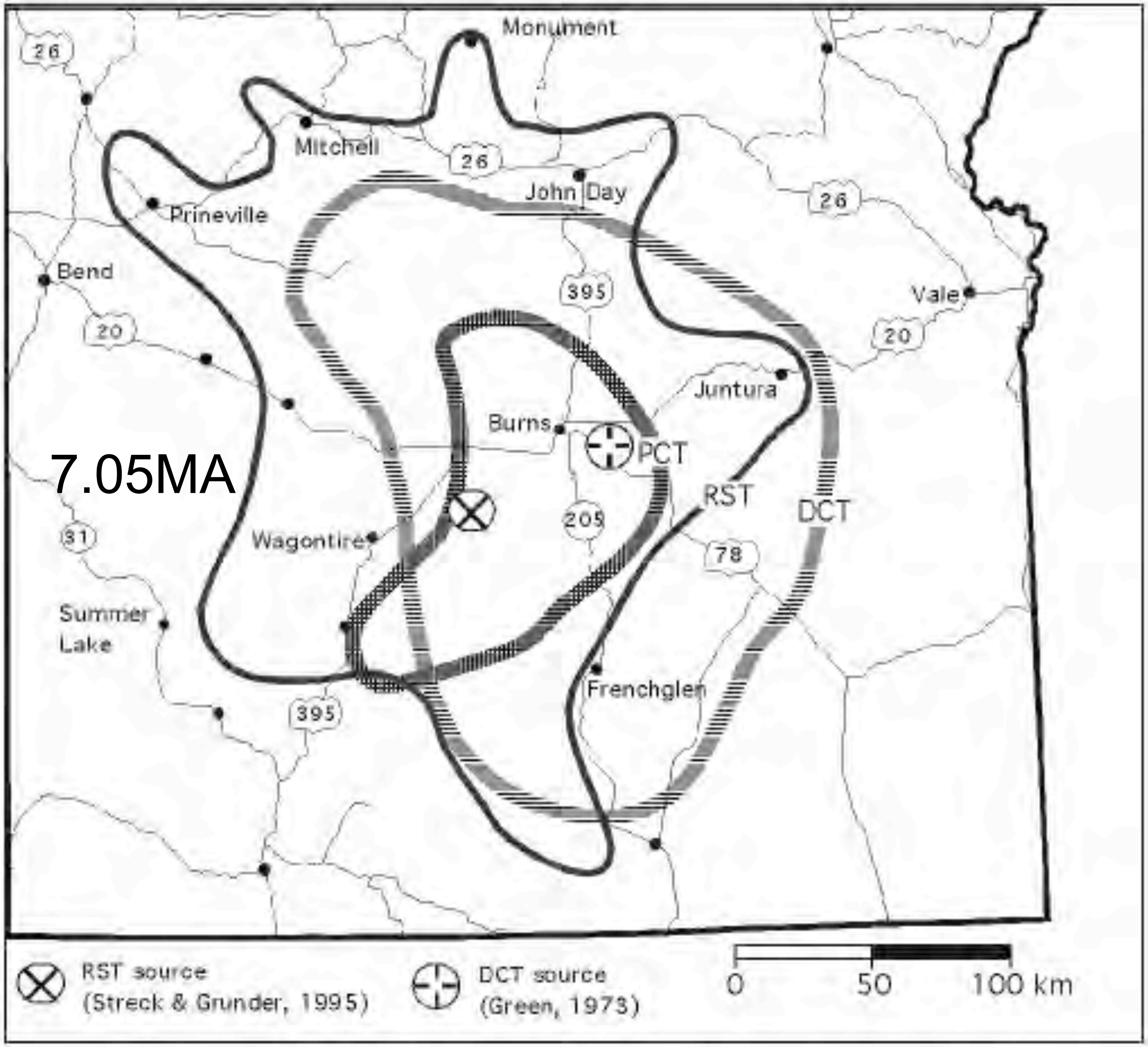


Figure 4. Inferred outlines and source areas of Harney Basin Tuffs. RST, Rattlesnake Tuff; PCT, Prater Creek Tuff; DCT, Devine Canyon Tuff. Outlines for DCT and PCT modified from Green (1973) and Walker (1979), respectively.

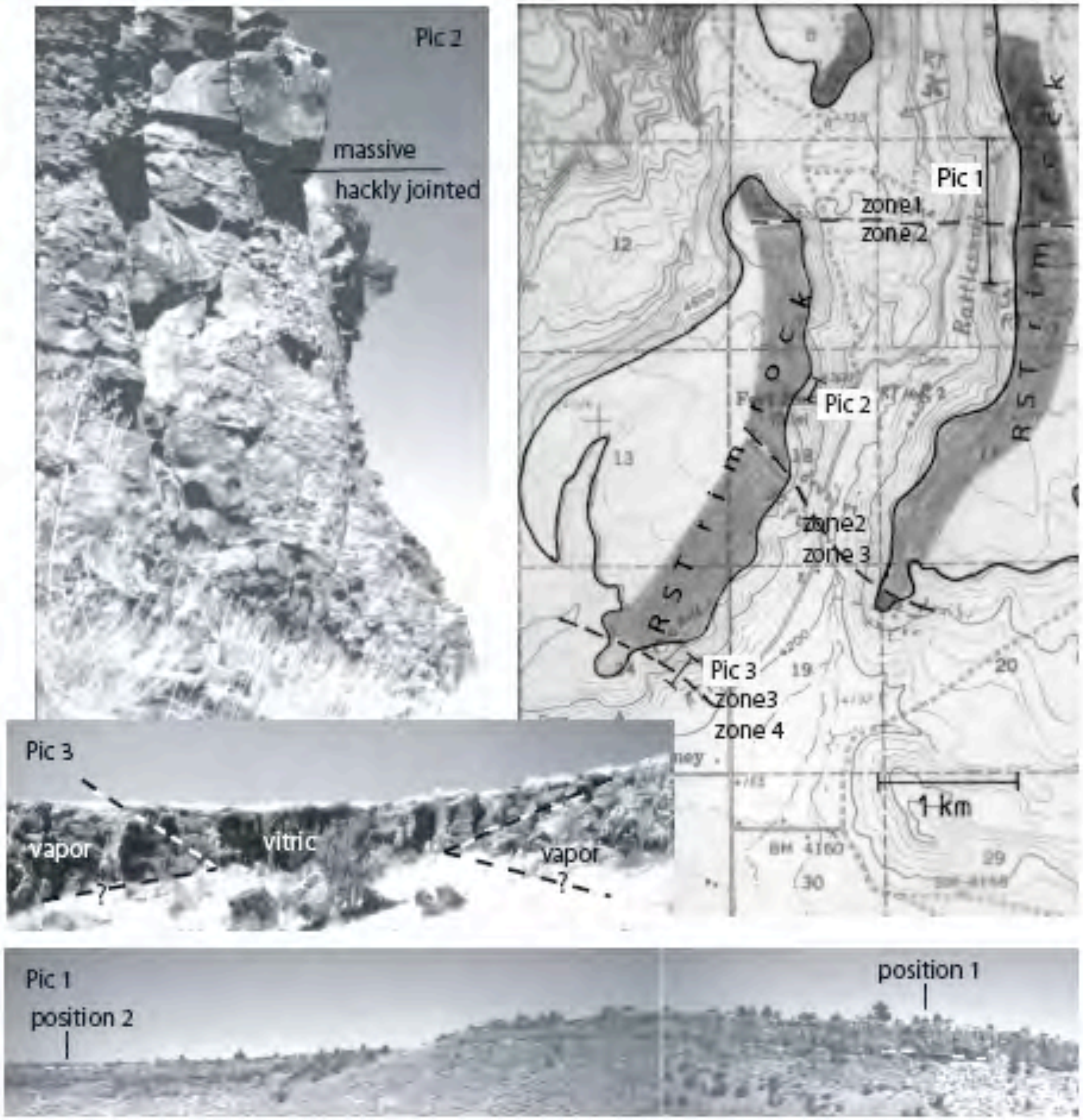


Figure 5. Overview of local facies changes. Zone 1: tuff dominated by thick lithophysal tuff underlying pervasively devitrified tuff and overlying (inferred, not exposed here) lower non- to densely welded vitric tuff. Zone 2: tuff dominated by pervasively devitrified tuff (Pic 2) overlying lower vitric tuff and underlying upper vitric tuff. Zone 3: tuff section consists of partially welded (with pumice) tuff that is vitric or vapor phase altered. Zone 4: vitric incipiently welded tuff. Picture 1: at position 1, densely welded vitrophyre exposed below white dashed line and section is topped with float of upper vitric tuff and at position 2, entire section below white dashed line is lithophysal tuff. Picture 2 shows pervasively devitrified tuff throughout in two facies, hackly jointed and massive. Picture 3: in middle of picture, tuff consists entirely of vitric tuff (vitric) that splits into a lower and upper vitric tuff separated by vapor phase tuff (vapor) further to the right and left, dashed lines indicate position of sharp interfaces between vitric and vapor phase tuff (analogous to the one seen in fig. 13 in Streck and Grunder, 1995).

# Rattlesnake Tuff Outcrops

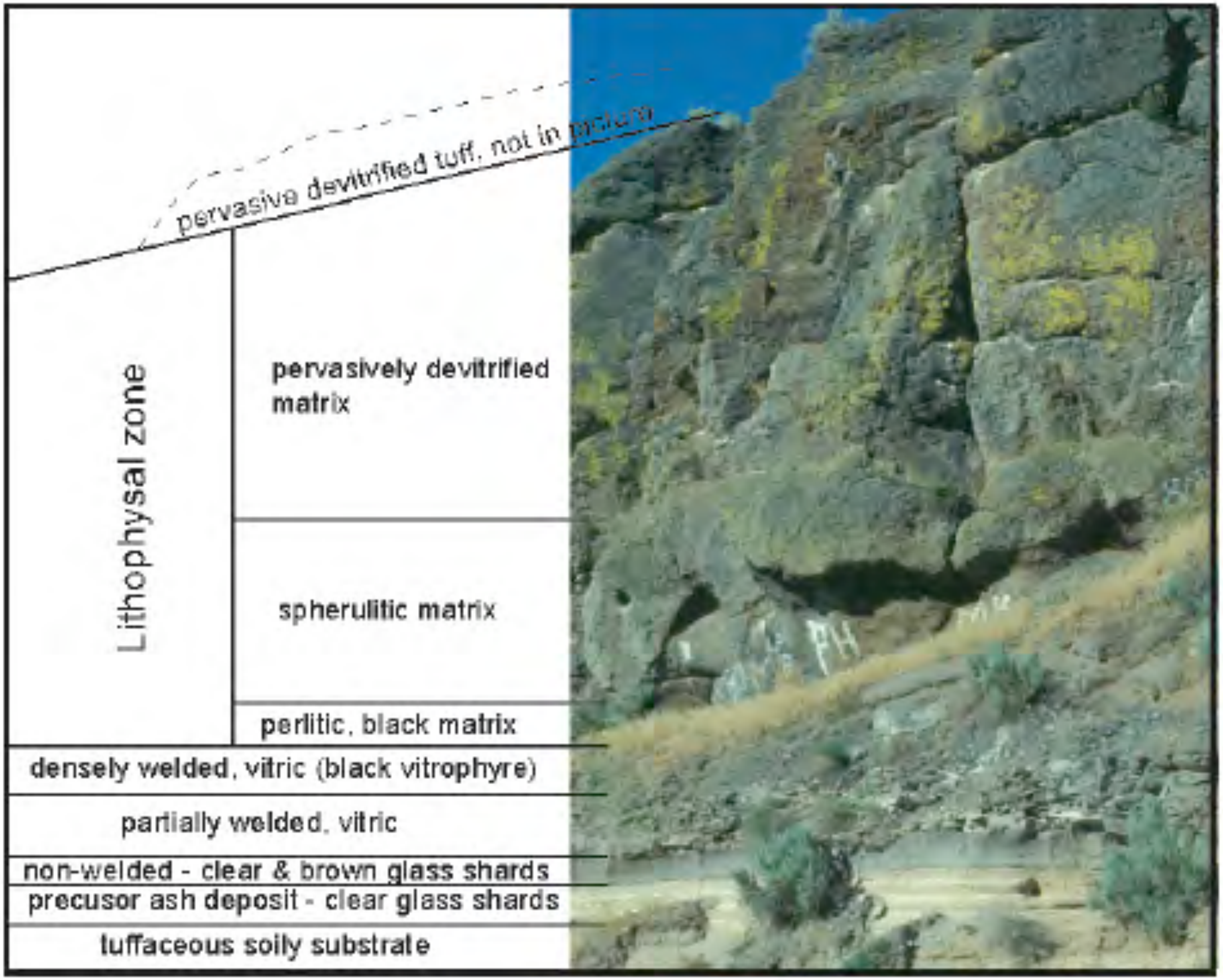


Figure 6. Outcrop stratigraphy of Rattlesnake Tuff at Stop 7.

# Type Locality Rattlesnake Tuff

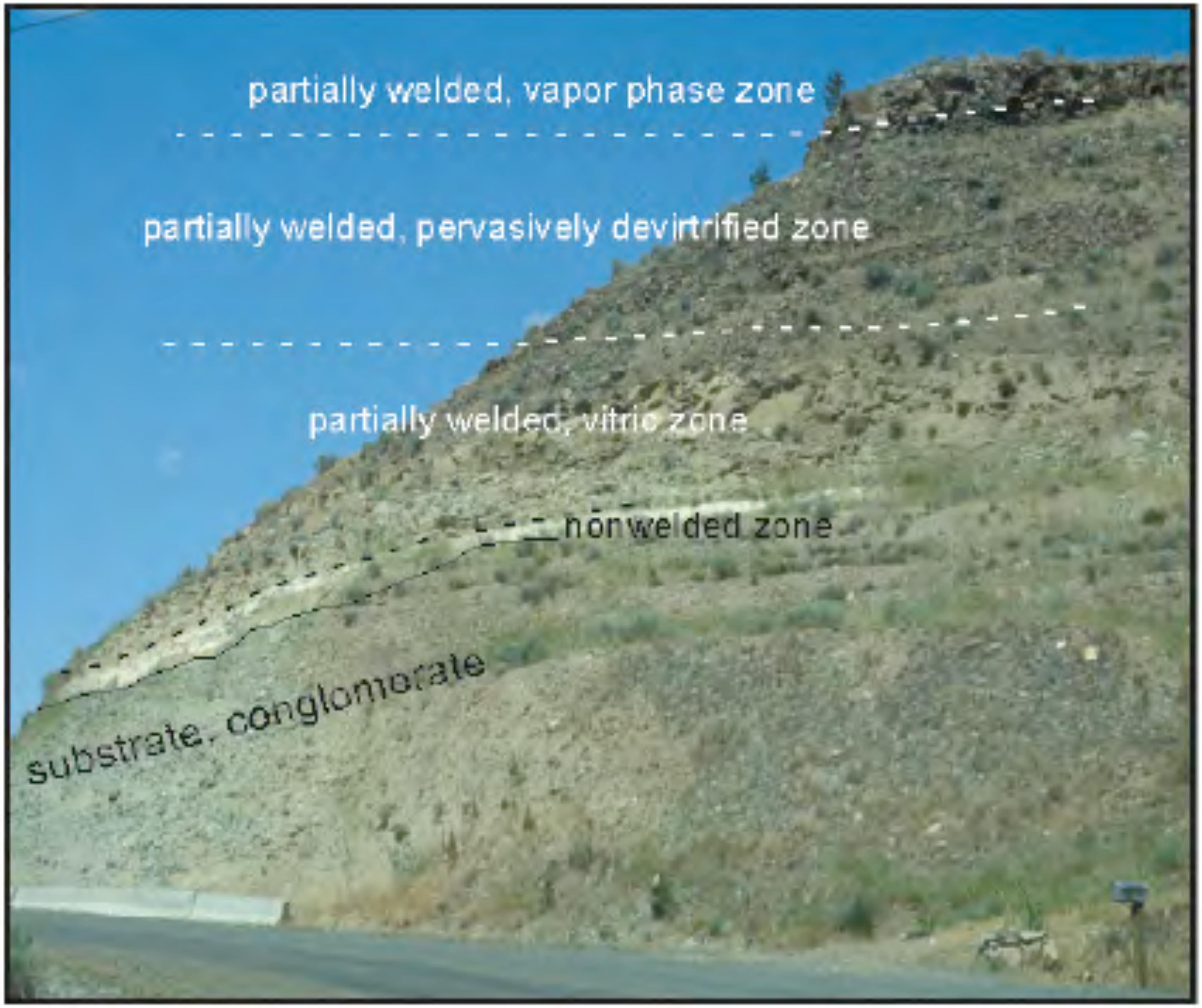


Figure 7. Outcrop stratigraphy of Rattlesnake Tuff at Stop 9.

Distal edge of Rattlesnake Tuff

# Miocene Flood Basalts

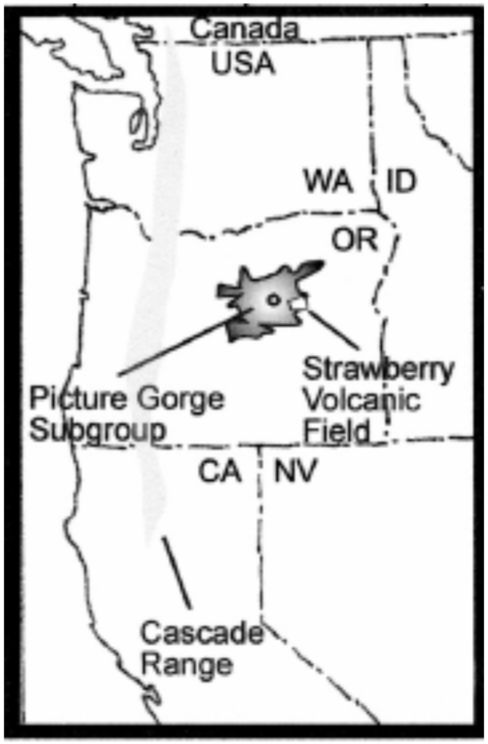


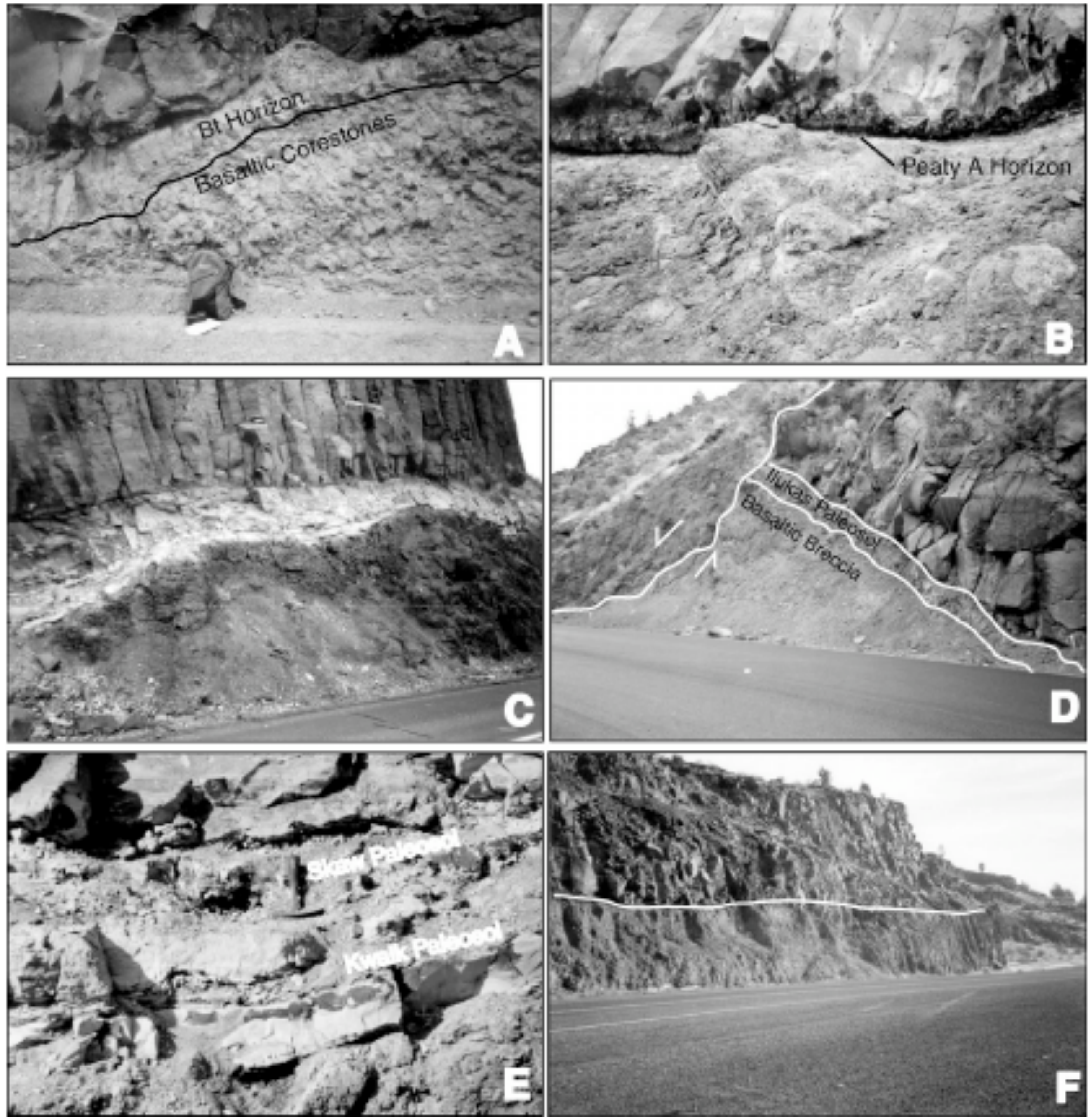


Picture Gorge Basalts from Sheldon (2003)

# Eastern Oregon Flood Basalts

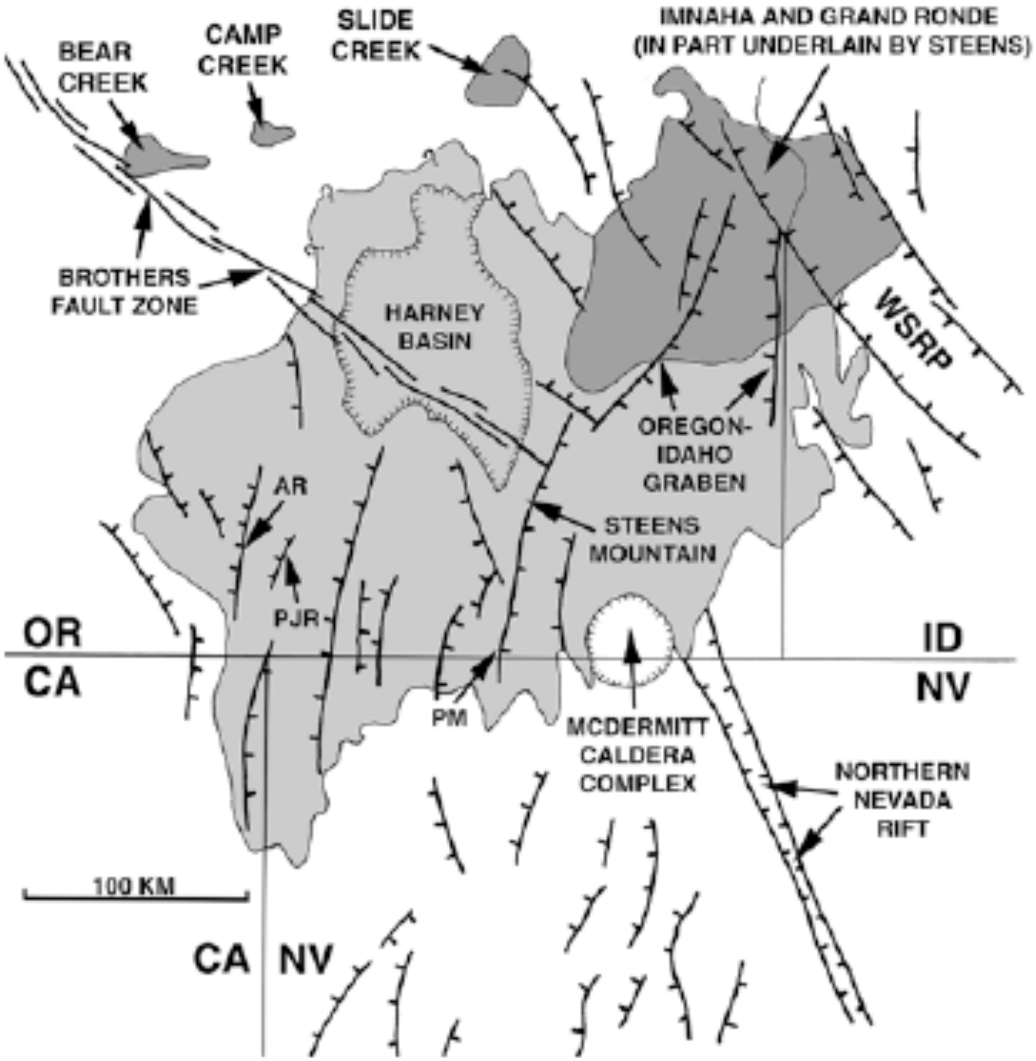


**Figure 1.** Approximate distribution of Miocene flood basalts in southeastern Oregon (~16.6–15.3 Ma). AR, Abert Rim; PJR, Poker Jim Ridge; PM, Pueblo Mountains, WSRP, Western Snake River Plain. See color version of this

CRB dikes in Wallow Granite

# Grande Ronde Flows and Dikes, Snake River

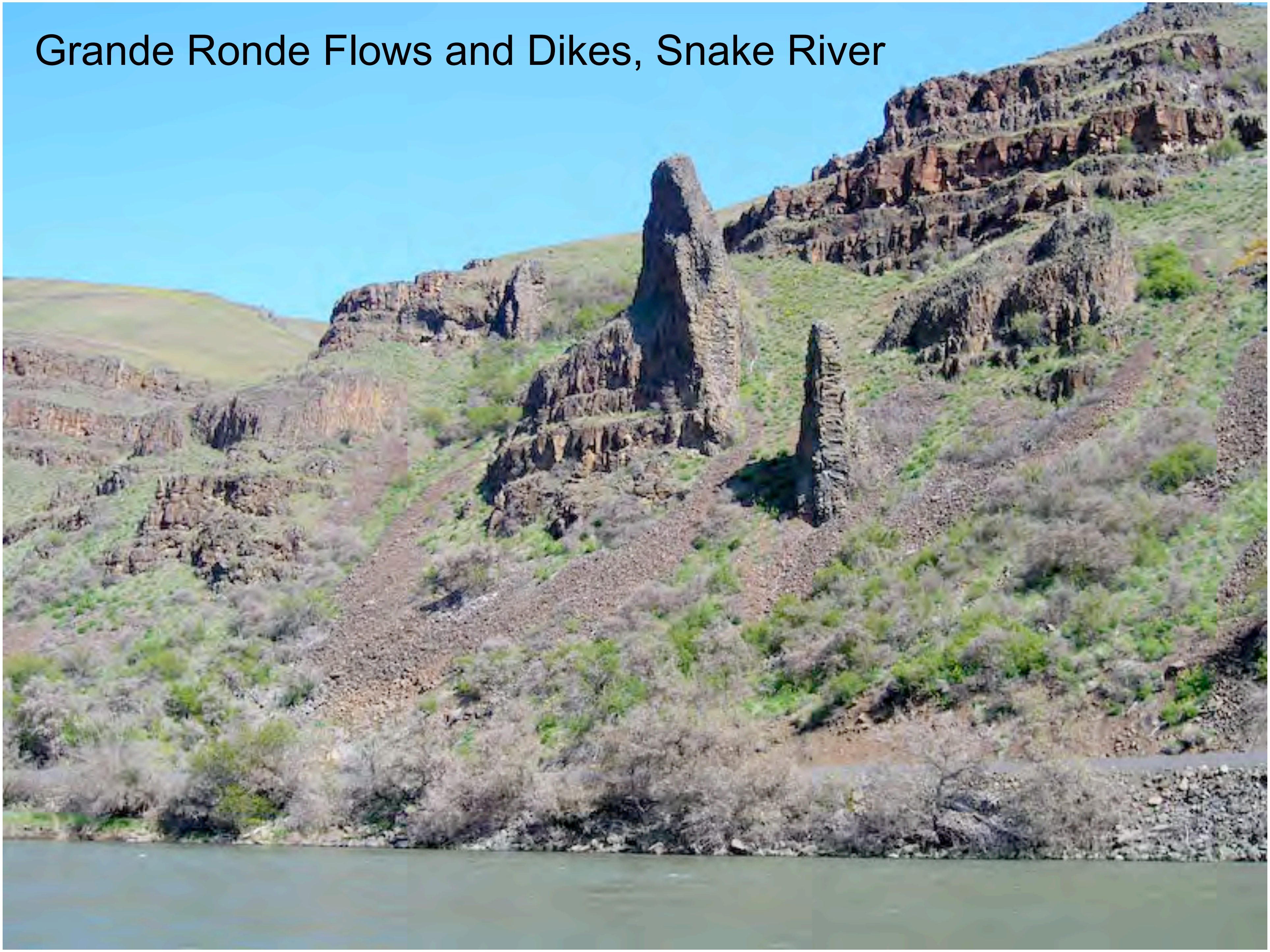

# Beeson et al 1985

| SERIES | | GROUP | SUB-GROUP | FORMATION | MEMBER | K-Ar AGE (m.y.) | MAGNETIC POLARITY |
|---|---|---|---|---|---|---|---|
| MIOCENE | UPPER | COLUMBIA RIVER BASALT GROUP | YAKIMA BASALT SUBGROUP | SADDLE MOUNTAINS BASALT | LOWER MONUMENTAL MEMBER | 6 | N |
| | | | | | *Erosional Unconformity* | | |
| | | | | | ICE HABOR MEMBER | 8.5 | |
| | | | | | Basalt of Goose Island | | N |
| | | | | | Basalt of Martindale | | R |
| | | | | | Basalt of Basin City | | N |
| | | | | | *Erosional Unconformity* | | |
| | | | | | BUFORD MEMBER | | R |
| | MIDDLE | | | | ELEPHANT MOUNTAIN MEMBER | 10.5 | R,T |
| | | | | | *Erosional Unconformity* | | |
| | | | | | POMONA MEMBER | 12 | R |
| | | | | | *Erosional Unconformity* | | |
| | | | | | ESQUATZEL MEMBER | | N |
| | | | | | *Erosional Unconformity* | | |
| | | | | | WEISSENFELS RIDGE MEMBER | | |
| | | | | | Basalt of Slippery Creek | | N |
| | | | | | Basalt of Lewiston Orchards | | N |
| | | | | | ASOTIN MEMBER | | N |
| | | | | | *Local Erosional Unconformity* | | |
| | | | | | WILBER CREEK MEMBER | | |
| | | | | | Basalt of Lapwai | | N |
| | | | | | Basalt of Wahluke | | N |
| | | | | | UMATILLA MEMBER | | |
| | | | | | Basalt of Sillusi | | N |
| | | | | | Basalt of Umatilla | | N |
| | | | | | *Local Erosional Unconformity* | | |
| | | | | WANAPUM BASALT | PRIEST RAPIDS MEMBER | 14.5 | |
| | | | | | Basalt of Lolo | | R |
| | | | | | Basalt of Rosalia | | R |
| | | | | | ROZA MEMBER | | T,R |
| | | | | | FRENCHMAN SPRINGS MEMBER | | |
| | | | | | Basalt of Lyons Ferry | | N |
| | | | | | Basalt of Sentinel Gap | | N |
| | | | | | Basalt of Sand Hollow | | N |
| | | | | | Basalt of Silver Falls | | N,E |
| | | | | | Basalt of Ginkgo | | E |
| | | | | | Basalt of Palouse Falls | | N |
| | | | | | ECKLER MOUNTAIN MEMBER | | |
| | | | | | Basalt of Shumaker Creek | | N |
| | | | | | Basalt of Dodge | | N |
| | | | | | Basalt of Robinette Mountain | | N |
| | LOWER | | | GRANDE RONDE BASALT | | 15.5 - 16.5 | $N_2$ |
| | | | | | | | $R_2$ |
| | | | | | | | $N_1$ |
| | | | | | | | $R_1$ |
| | | | | PICTURE GORGE BASALT | Basalt of Dayville<br>Basalt of Monument Mountain<br>Basalt of Twickenham | (14.6-15.8) | |
| | | | | IMNAHA BASALT | | 16.5 - 17.0 | $R_1$ |
| | | | | | | | T |
| | | | | | | | $N_0$ |
| | | | | | | | $R_0$ |

*Figure 1. Stratigraphic nomenclature, age, and magnetic polarity for the Columbia River Basalt Group, as revised by Swanson and others (1979b) and modified by the authors. N = normal magnetic polarity; R = reversed magnetic polarity; T = transitional magnetic polarity; E = excursional magnetic polarity.*

| MACKIN (1961, p.8) | BENTLEY (1977a, p.361) | BENTLEY AND CAMPBELL (1983) | THIS PAPER |
|---|---|---|---|
| | | | BASALT OF LYONS FERRY |
| SENTINEL GAP FLOW | UNION GAP FLOWS | FLOWS OF UNION GAP | BASALT OF SENTINEL GAP |
| SAND HOLLOW FLOW | KELLEY HOLLOW FLOWS<br>SAND HOLLOW FLOWS<br>MARY HILL FLOW | FLOW OF KELLEY HOLLOW†<br>FLOW OF BADGER GAP** | BASALT OF SAND HOLLOW*<br>BASALT OF SILVER FALLS |
| GINKGO FLOW | GINKGO FLOW | GINKGO FLOWS | BASALT OF GINKGO |
| | PALOUSE FALLS FLOW | | BASALT OF PALOUSE FALLS |

† Equivalent to the Sand Hollow and Sentinel Gap Flows of Mackin (1961)
** Sand Hollow Flow of Bentley (1977a)
* Includes Basalt of Sheffler (Swanson and others, 1980)

*Figure 2. Chart showing correlation of previously defined units of the Frenchman Springs Member to those of this paper.*

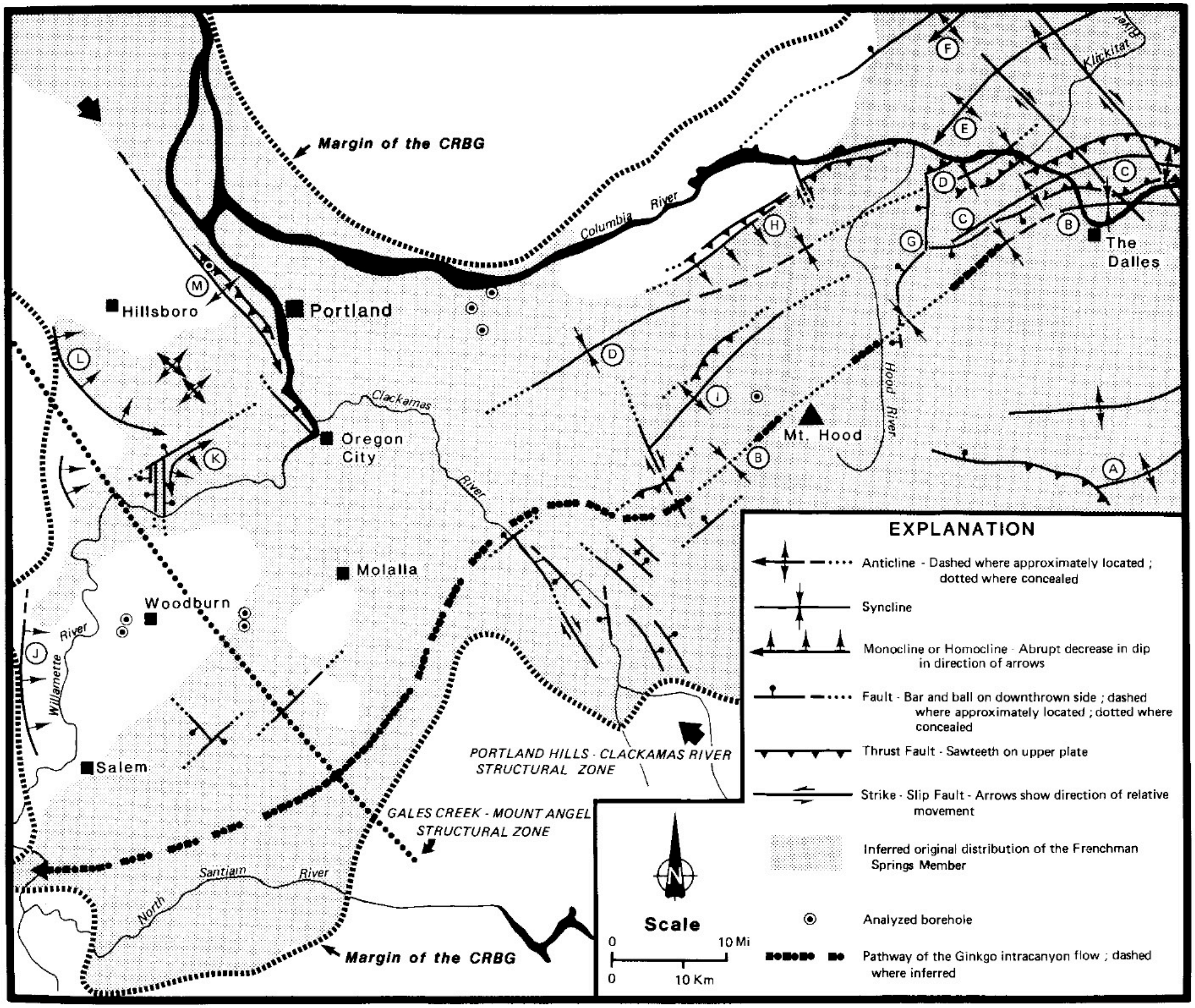


*Figure 6. Generalized sketch map showing selected major structures in western Oregon and Washington and the pathway of the Ginkgo intracanyon flow. Structural features shown include the following: A = Tygh Ridge; B = Dalles-Mount Hood syncline; C = Columbia Hills; D = Mosier-Bull Run syncline; E = Bingen anticline; F = Horse Heaven Hills-Simcoe Mountains uplift; G = Hood River fault zone; H = Eagle Creek homocline; I = Bull Run anticline; J = Eola Hills homocline; K = Parrett Mountain structure; L = Chehalem Mountain homocline; M = Portland Hills anticline.*

Beeson et al 1985

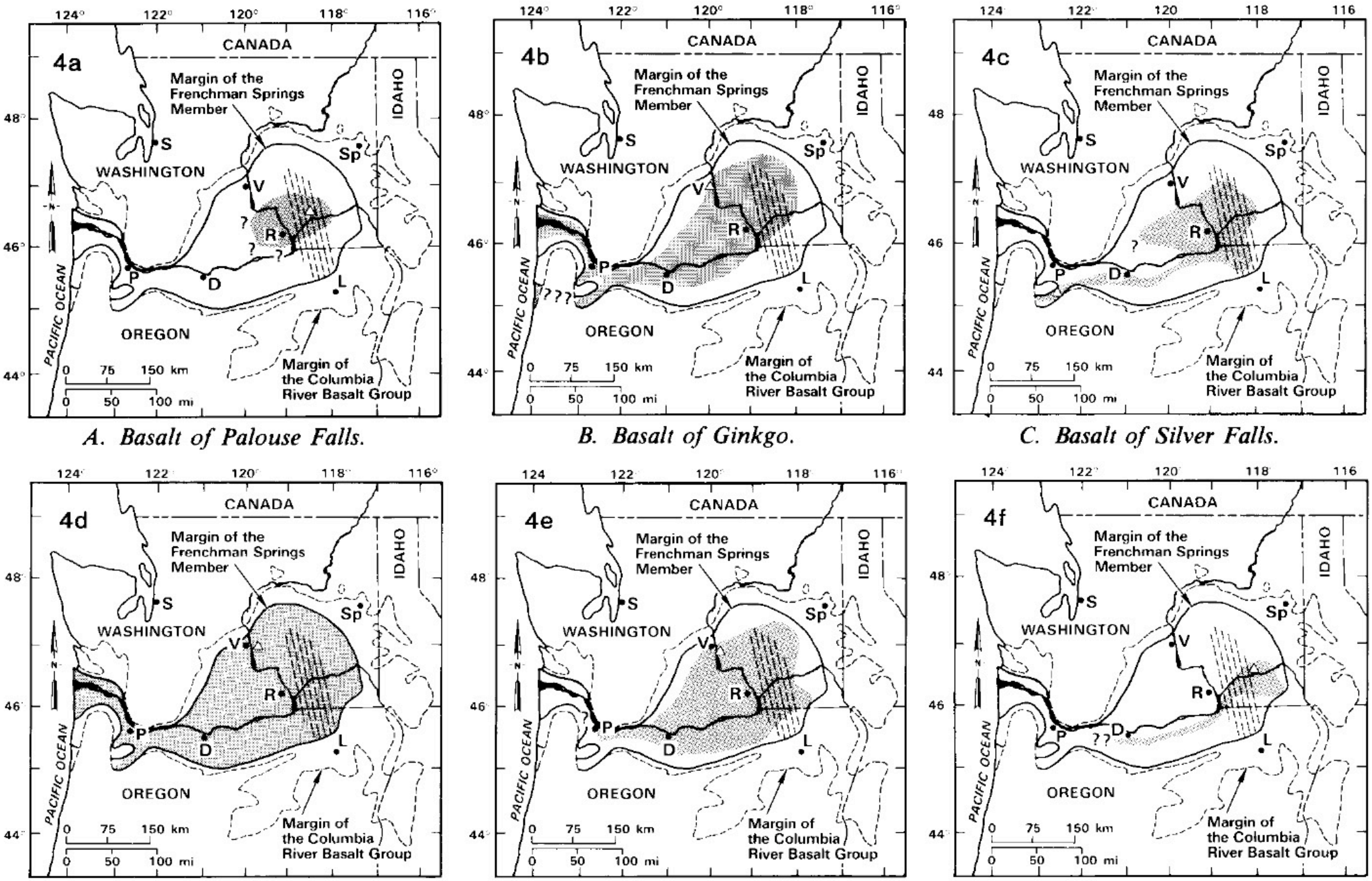


A. *Basalt of Palouse Falls.* B. *Basalt of Ginkgo.* C. *Basalt of Silver Falls.*

D. *Basalt of Sand Hollow.* E. *Basalt of Sentinel Gap.* F. *Basalt of Lyons Ferry.*

*Figure 4. Maps showing inferred original extent (stippled areas) of units of the Frenchman Springs Member defined in this paper. Known and inferred dike and vent areas are shown schematically by parallel dashed lines. Locations of type localities are designated by open triangles. Cities: Sp = Spokane; L = La Grande; R = Richland; V = Vantage; D = The Dalles; S = Seattle; P = Portland.*

Beeson et al 1985

# Genesis of flood basalts … from Steens Mountains to the Malheur River Gorge, Oregon

Camp et al 2003

GSA Bulletin pp. 105-128.

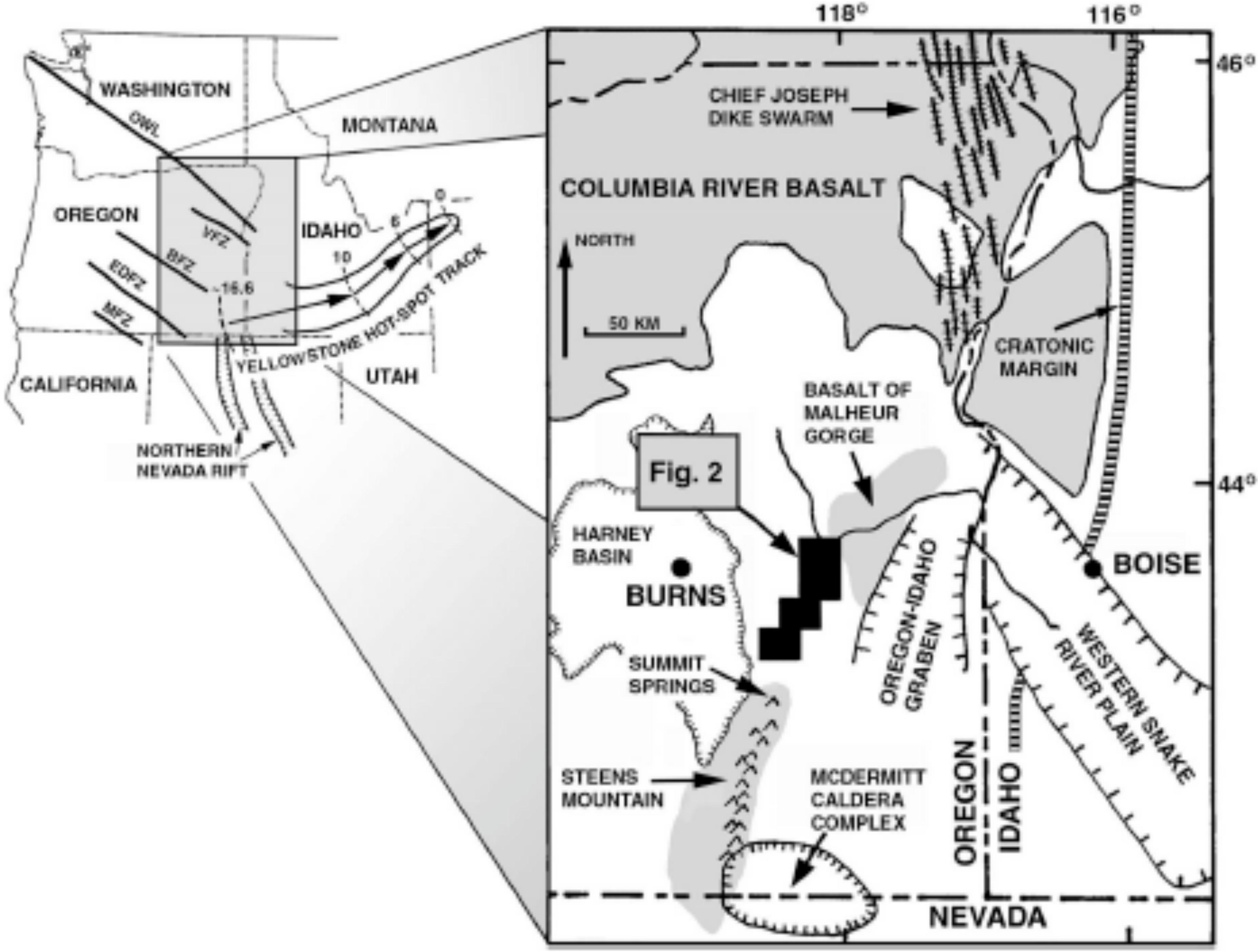

WASHINGTON
MONTANA
OREGON
IDAHO
CALIFORNIA
UTAH
OWL
VFZ
BFZ
EDFZ
MFZ
16.6
10
6
0
YELLOWSTONE HOT-SPOT TRACK
NORTHERN NEVADA RIFT
118°
116°
46°
44°
CHIEF JOSEPH DIKE SWARM
COLUMBIA RIVER BASALT
NORTH
50 KM
CRATONIC MARGIN
BASALT OF MALHEUR GORGE
Fig. 2
HARNEY BASIN
BURNS
BOISE
OREGON-IDAHO GRABEN
WESTERN SNAKE RIVER PLAIN
SUMMIT SPRINGS
STEENS MOUNTAIN
MCDERMITT CALDERA COMPLEX
OREGON
IDAHO
NEVADA

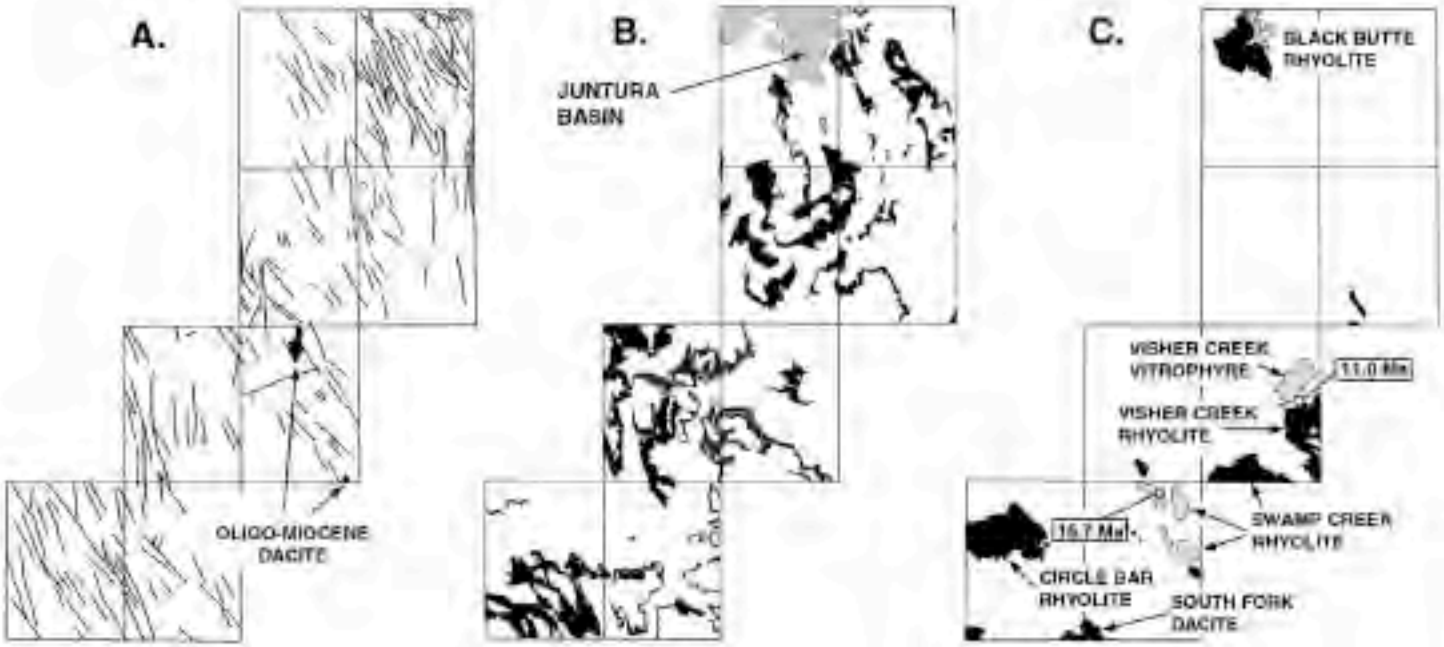


Figure 3. Aspects of the general geology. (A) Overall fault pattern and distribution of the Oligocene–Miocene volcanic rocks. (B) Distribution of the undifferentiated Miocene pyroclastic rocks and pyroclastic sediments, spanning an age range from ca. 15.0 and 7.0 Ma. (C) Distribution of the shallow felsic eruptive centers. Outflow facies of ignimbrite or vitrophyric lava are shown by dotted pattern. Radiometric dates for the Swamp Creek and Visher Creek rhyolites are from Walker (1979).

| Extension / volcanism | Graben | VOLCANIC SUCCESSION | | VOLCANIC UNIT | AGE | COMMENT |
|---|---|---|---|---|---|---|
| BASIN AND RANGE EXTENSION | | Late Diktytaxitic Olivine Basalts | | Voltage flow | 32 ka | A |
| | | | | Drinkwater basalt | ca. 7.0 Ma | B |
| | | *Regional Unconformity* | | | | |
| | | Intermediate to Felsic Calc-alkaline Rocks | | Devine Canyon tuff | ca. 9.7 Ma | C |
| | | | KEENEY SEQUENCE | Cobb Creek lavas | — | — |
| | | | | Riverside lavas | 10.14 ± 0.23 Ma | D |
| | | | | Buck Mtn. lavas | 12.5 ± 0.5 Ma | E |
| | | *Regional Unconformity* | | | | |
| FLOOD BASALT VOLCANISM | Opening of Oregon-Idaho Graben | Early Diktytaxitic Olivine Basalts | | Tims Peak basalt | 13.5 ± 0.1 Ma | F |
| | | *Regional Unconformity* | | | | |
| | | Tholeiitic Mafic to Bimodal Rocks | | Hunter Creek basalt | 15.3 ± 0.1 Ma | F,G |
| | | | | Dinner Creek tuff | | |
| | | | | Kool Spring fm. | — | — |
| | | | | Steens basalt, Venator Ranch basalt, and basalt of Malheur Gorge | 15.7 ± 0.1 Ma | F,G |
| | | | | | | — |
| | | | | | 16.6 ± 0.02 Ma | H |
| | | *Regional Unconformity* | | | | |
| | | Oligo-Miocene dacite | | | ca. 23.7-17.8 Ma | I |

ic stratigraphy along the middle and south forks of the Malheur River, Oregon, is subdivided b
l by well-developed unconformities. Comments on age designations: (A) Gehr and Newman (

Figure 5. Dike of Venator Ranch basalt cutting across Oligocene–Miocene volcanic rocks in the McEwen Butte Quadrangle, 7 km south of Riverside, Oregon.

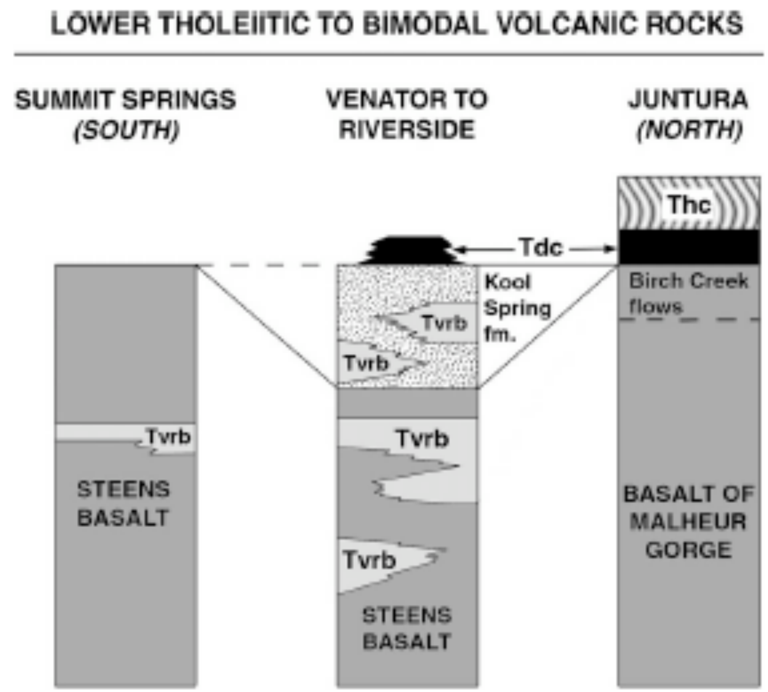


in the north. Throughout most of this region, the upper part of the Steens sequence is interbedded with a group of previously unrecognized tholeiitic lavas, herein referred to as the Venator Ranch basalt. The interbedded succession of Steens and Venator Ranch basalts is in turn overlain by an interbedded bimodal succession of air-fall pyroclastic deposits and Venator Ranch basalt flows, herein called the Kool Spring formation (Figs. 4). Two small

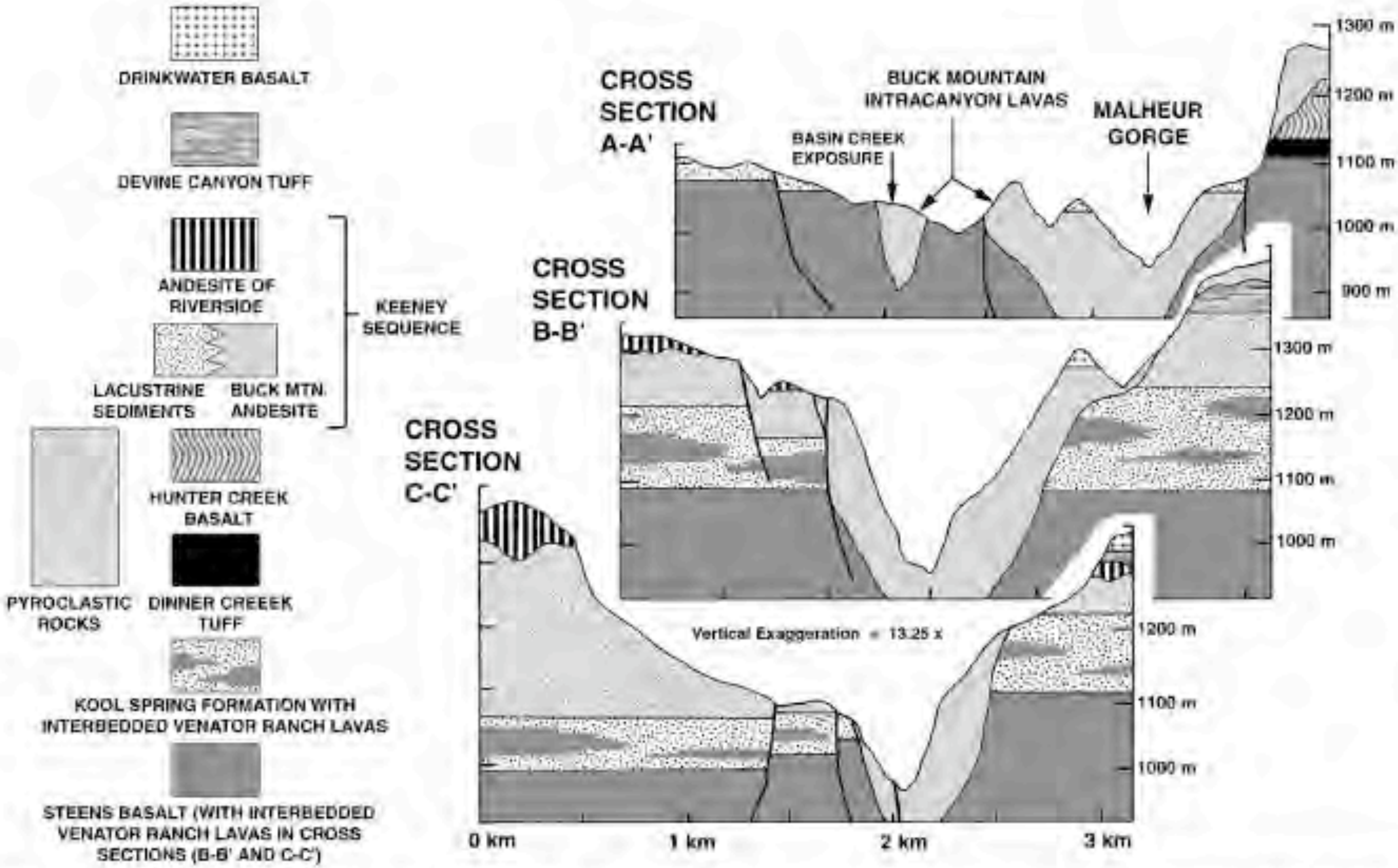


Figure 9. Stratigraphic cross sections across the middle fork of the Malheur River, south of Juntura and north of Riverside (for locations, see Fig. 8). The current channel of the middle fork follows the Miocene channel of the ancestral Malheur River, which was filled with Buck Mountain lava flows up to 500 m thick.

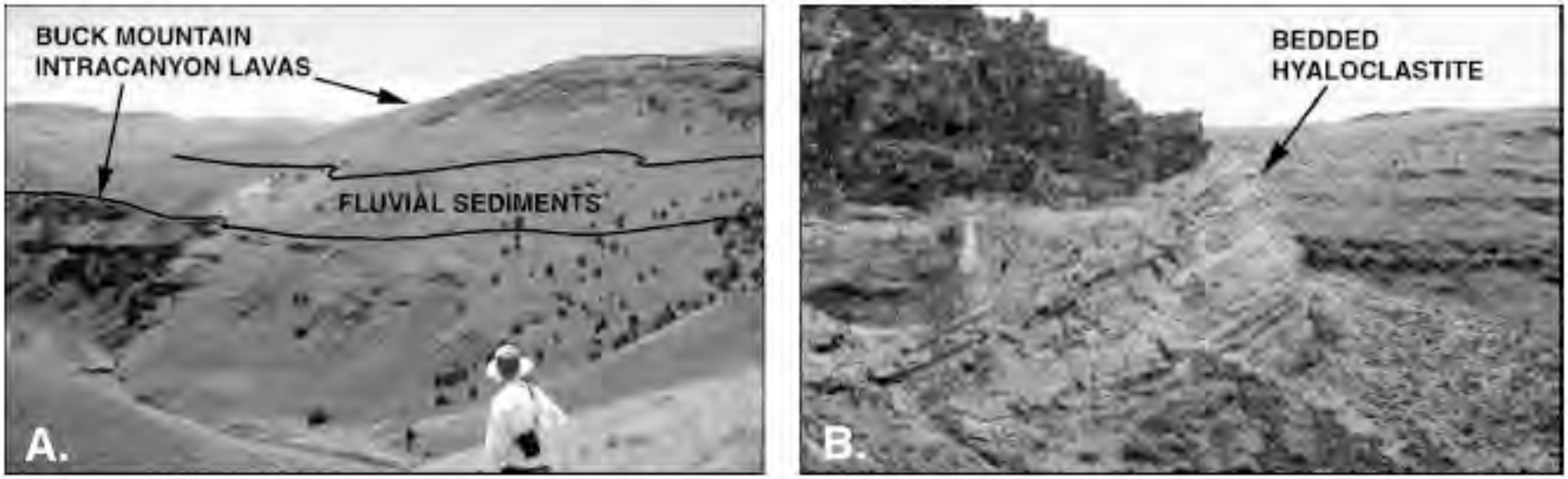


Figure 10. Buck Mountain intracanyon lavas with interbedded sediments and hyaloclastite. (A) Buck Mountain intracanyon lava flows exposed along the eastern flank of Meeker Mountain (top) and along the western canyon wall of the middle fork of the Malheur River (bottom), ~13 km south of Juntura. Distinct lava flows are separated by lensoid sedimentary interbeds, generated by the periodic disruption of the ancestral Malheur River. The thickest of these deposits is a 40-m-thick deposit of water-laden tuffaceous sediments and fluvial gravels exposed on the bench separating the upper and lower lava successions. (B) Reworked, bedded hyaloclastite deposit separating two intracanyon Buck Mountain lava flows filling a steep-walled ancestral valley, well exposed in Basin Canyon (see cross section A–A′, Fig. 9).

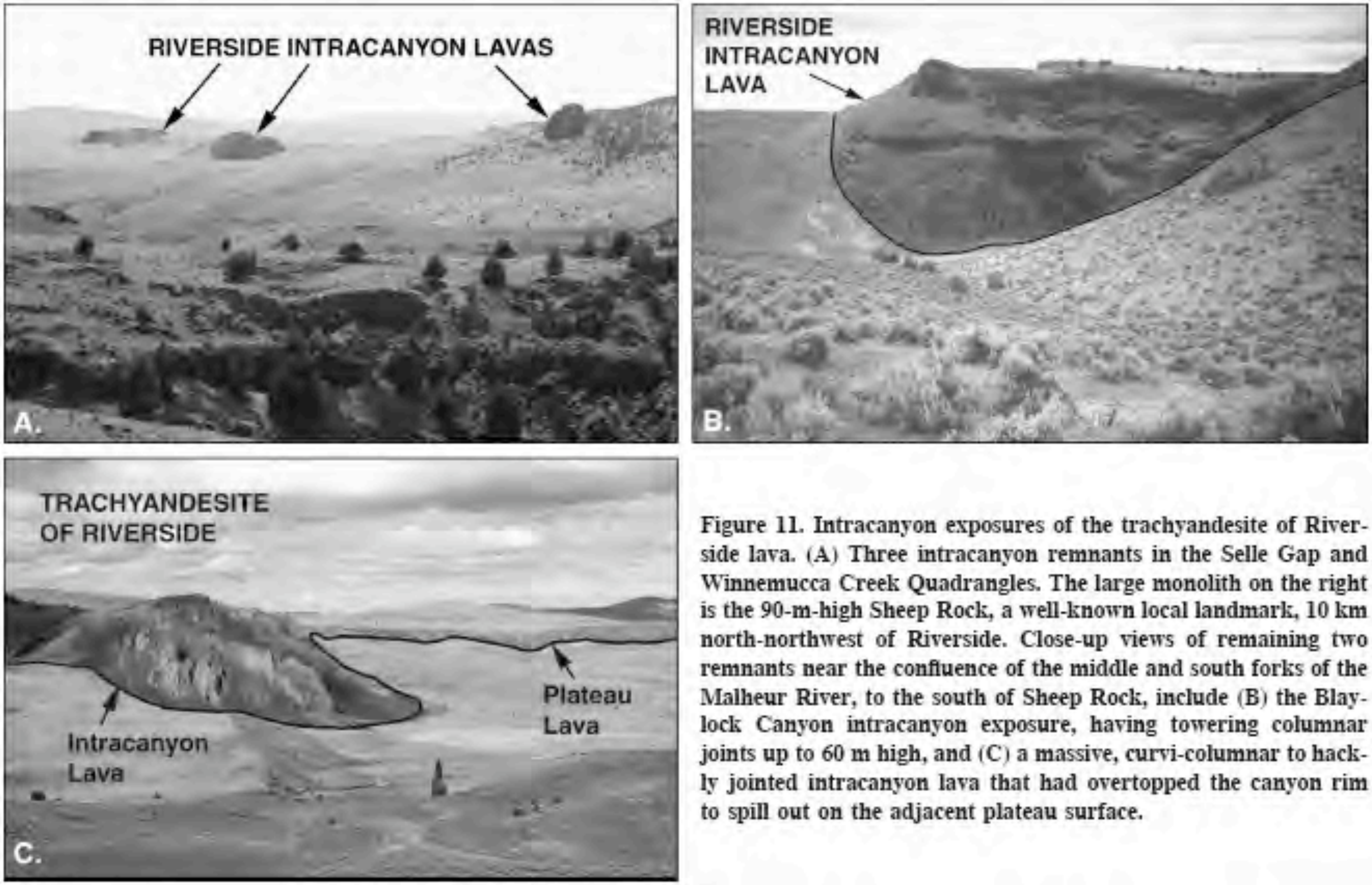


Figure 11. Intracanyon exposures of the trachyandesite of Riverside lava. (A) Three intracanyon remnants in the Selle Gap and Winnemucca Creek Quadrangles. The large monolith on the right is the 90-m-high Sheep Rock, a well-known local landmark, 10 km north-northwest of Riverside. Close-up views of remaining two remnants near the confluence of the middle and south forks of the Malheur River, to the south of Sheep Rock, include (B) the Blaylock Canyon intracanyon exposure, having towering columnar joints up to 60 m high, and (C) a massive, curvi-columnar to hackly jointed intracanyon lava that had overtopped the canyon rim to spill out on the adjacent plateau surface.

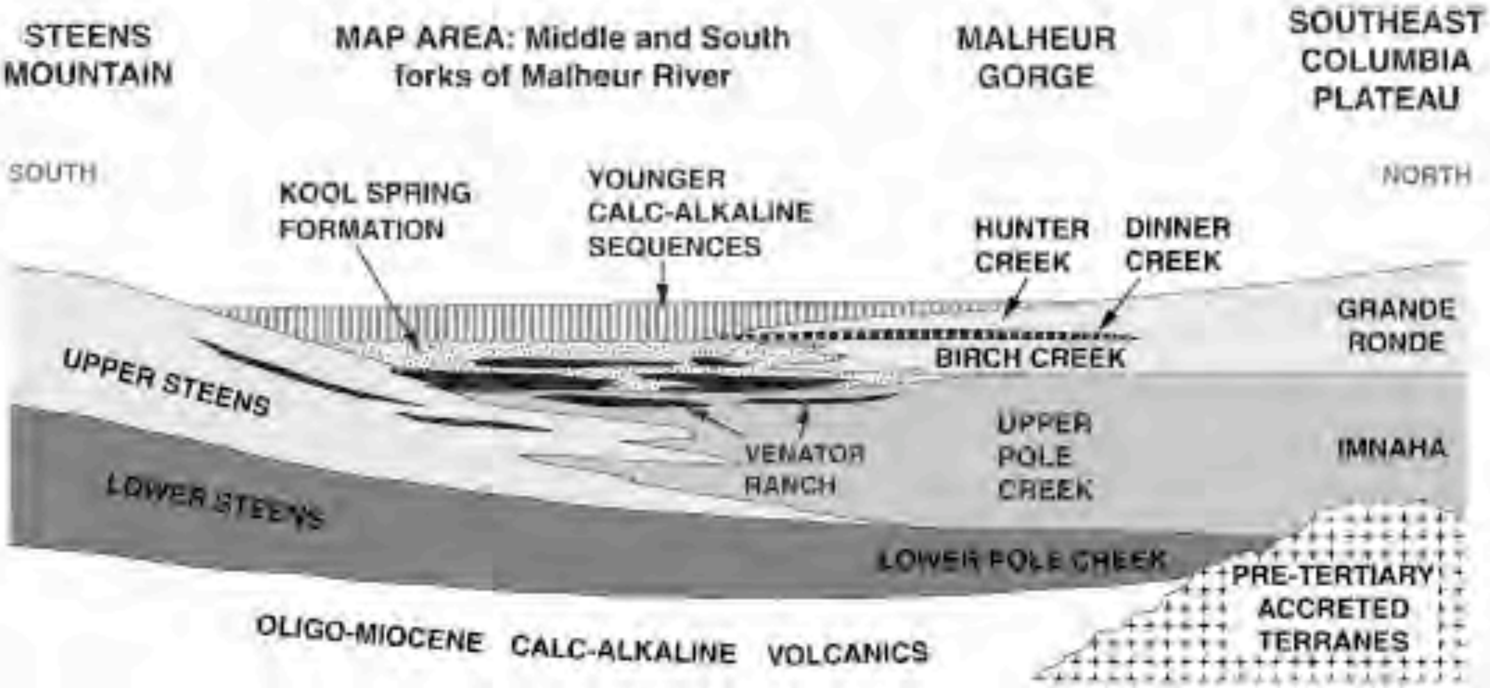


Figure 20. Generalized schematic cross section from Steens Mountain in the south, through the map area, to the Columbia Plateau in the north. Regional stratigraphic relationships are based on the mapping and petrochemical data presented here and on a variety of mapping and petrochemical studies summarized in Hooper et al. (2002a).

# Mantle dynamics and genesis of mafic magmatism in the intermontane Pacific Northwest

Camp and Ross 2004

JGR pp B08204-B08228

# Miocene Columbia River Basalts


**Figure 2.** New distribution map for the Columbia River Flood Basalt Province. MC, McDermitt caldera; OIG, Oregon-Idaho graben; WSRP, Westem Snake River Plain.

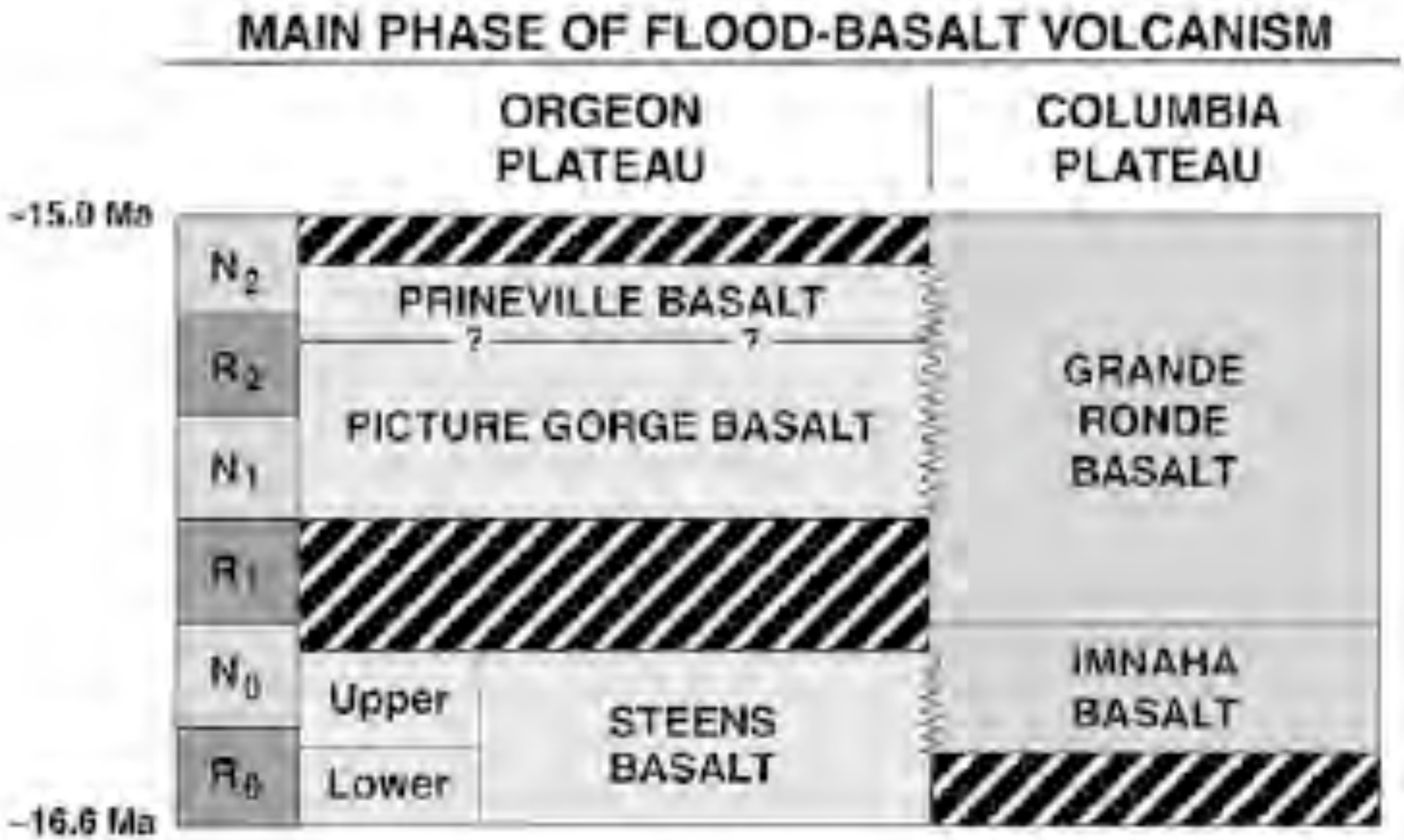


**Figure 4.** Magnetostratigraphy of flood basalt units on the Columbia and Oregon Plateaus during the main phase of flood basalt eruption (~16.6–15.0 Ma). See color version

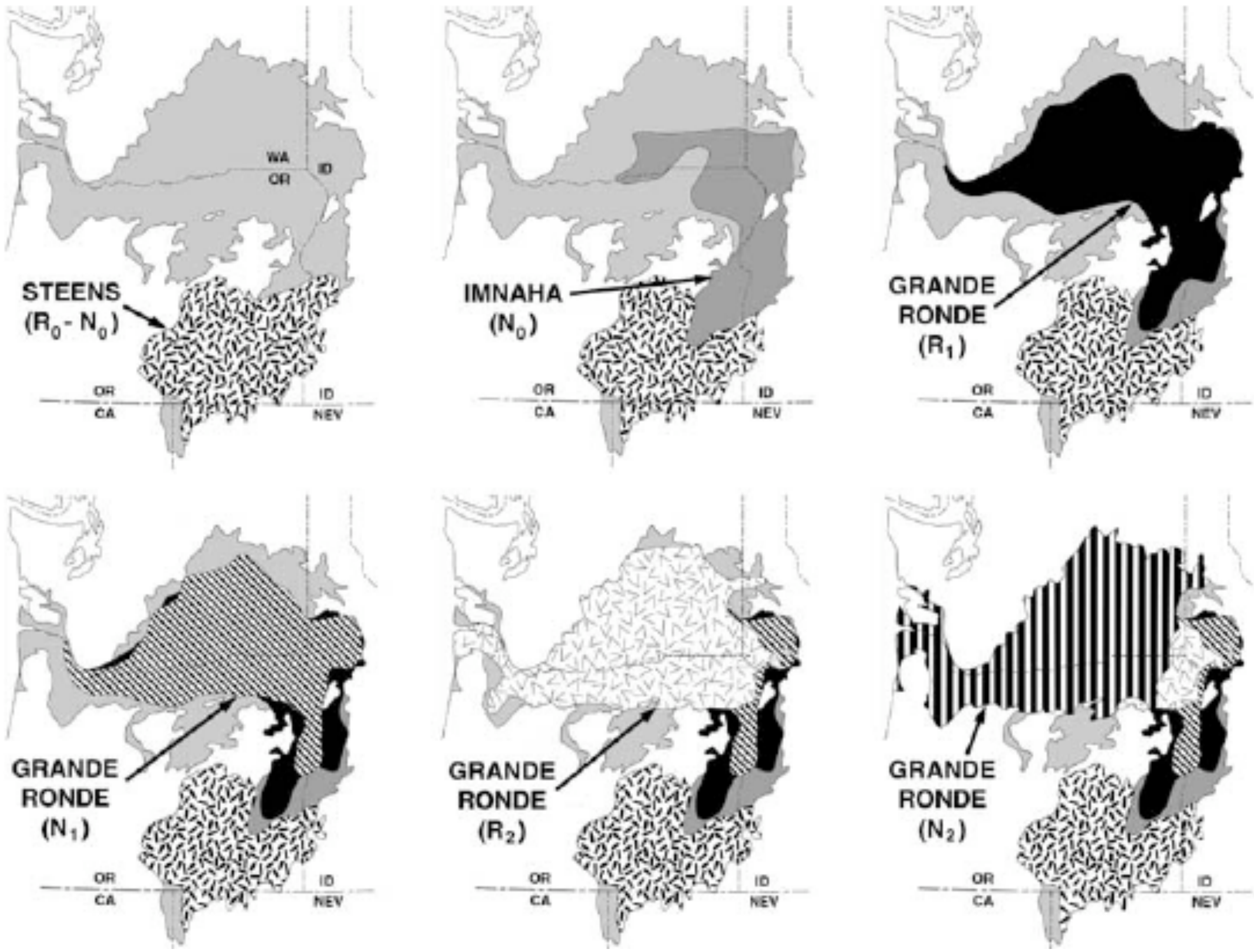


**Figure 5.** Age-progressive distribution of Steens basalt, Imnaha Basalt, and each of the Grande Ronde magnetostratigraphic units erupting from the Chief Joseph dike swarm. See color version of this figure in

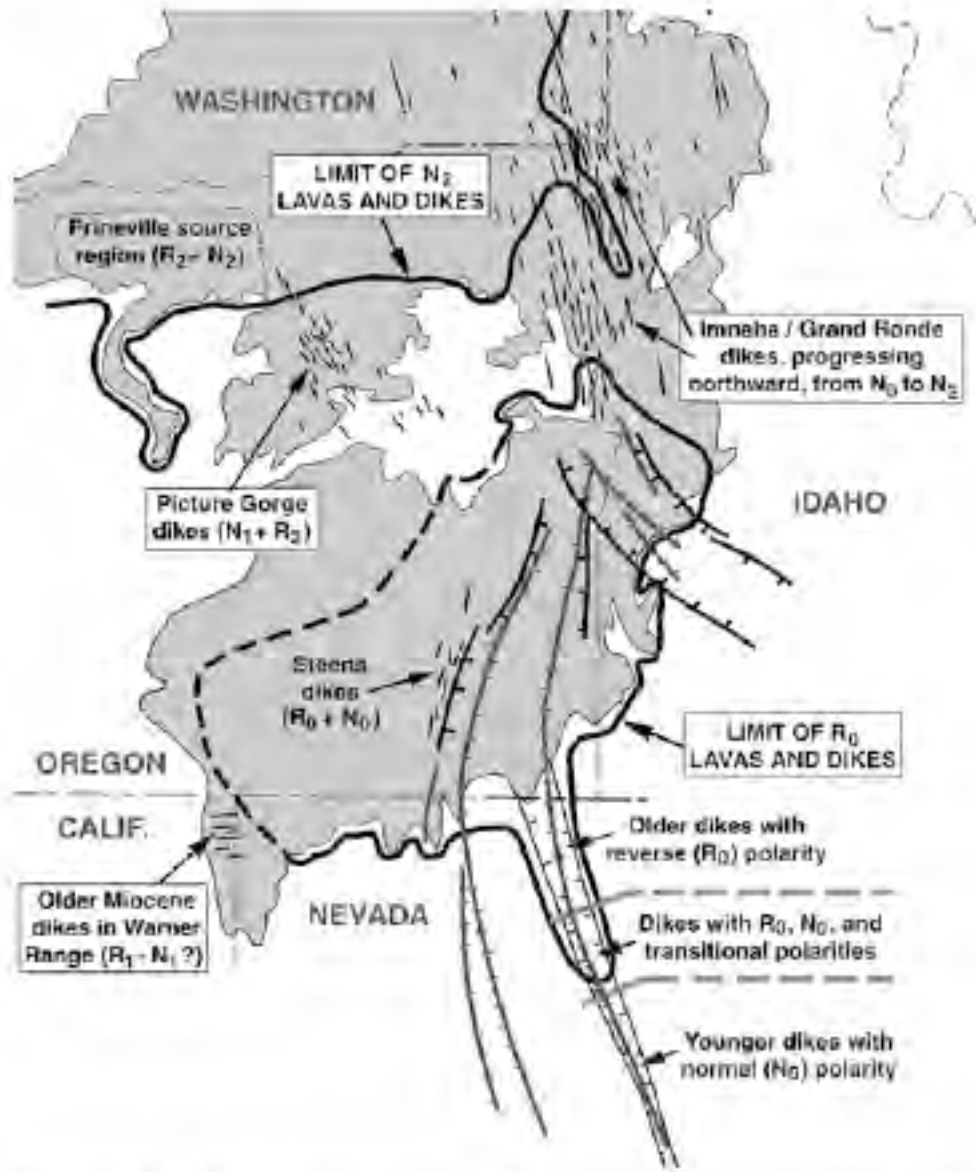


**Figure 6.** Map showing (1) the eruption sites of Columbia River Basalt volcanism, (2) the restricted areal extent of $R_0$ lavas and dikes, and (3) the southern extent of $N_2$ lavas and dikes associated with the main phase of eruption.

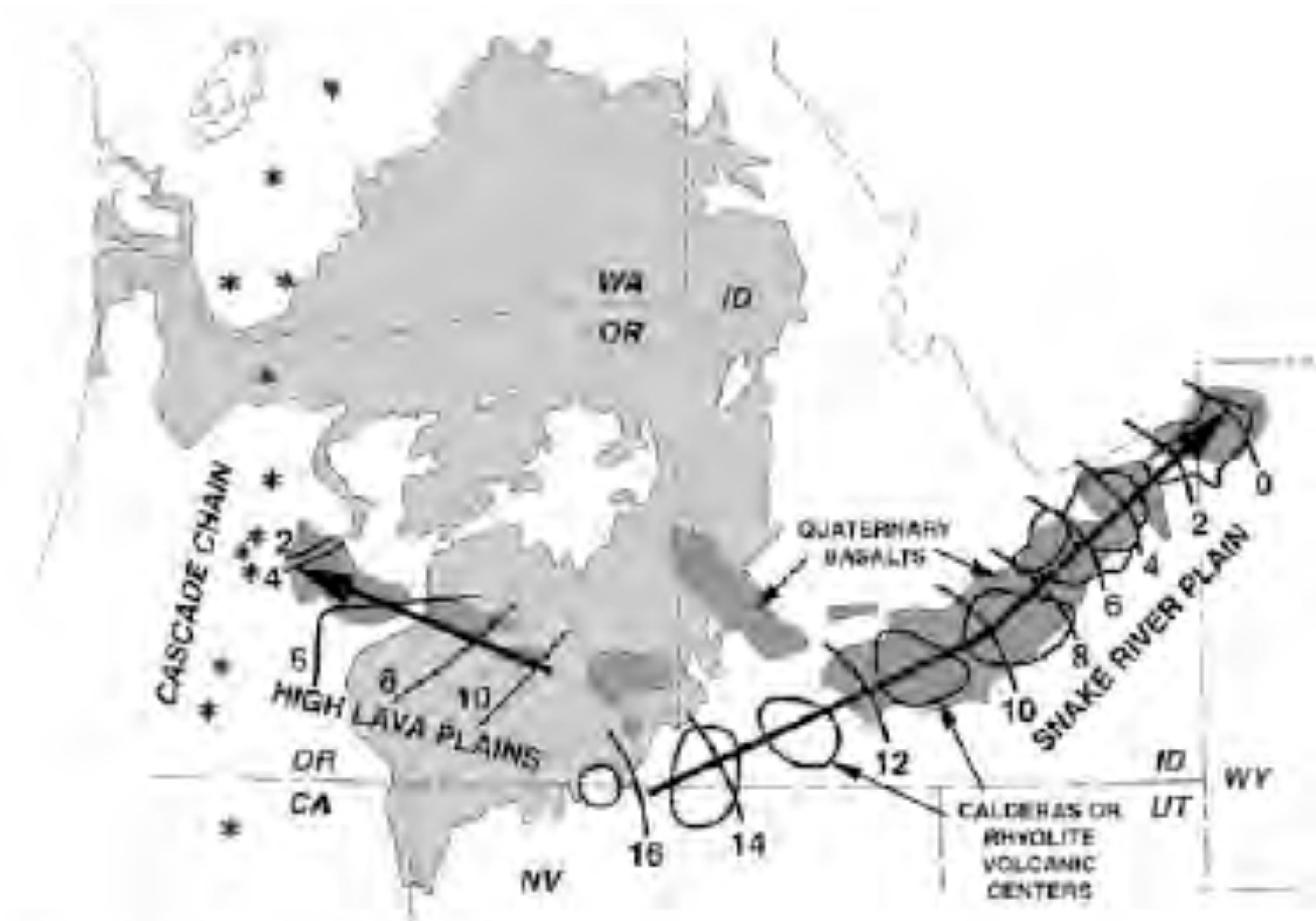


**Figure 7.** Moderate rate migrations of rhyolite magmatism associated with the Oregon High Lava Plains and the Snake River Plain hot spot track. Distribution of Quaternary basalt outcrops are from *Christiansen et al.* [2002]. Isochrons for rhyolitic volcanism are from *Jordan et al.* [2002] and *Christiansen et al*. [2002]. See color version of this figure in

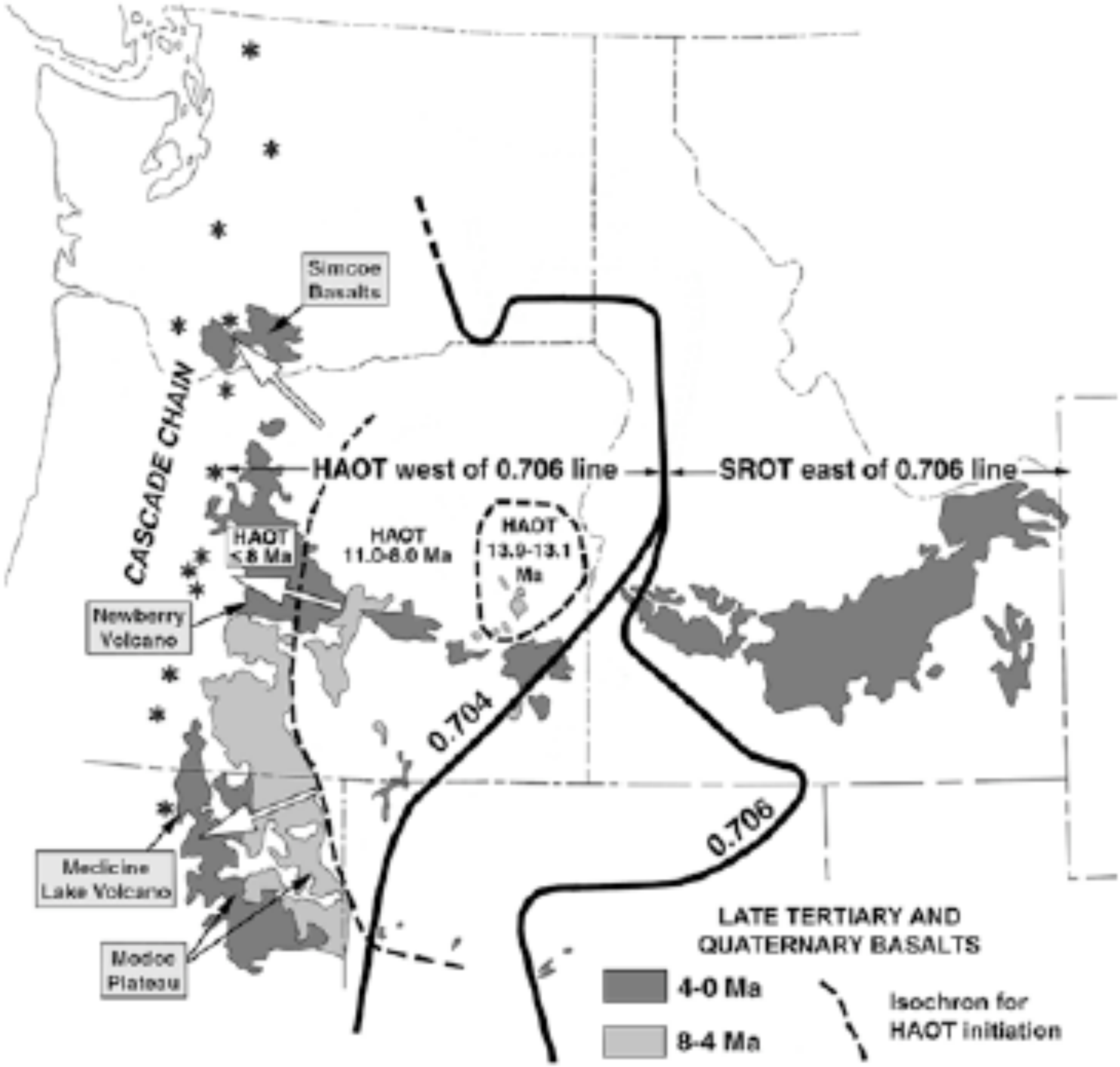

Simcoe Basalts
CASCADE CHAIN
HAOT west of 0.706 line
SROT east of 0.706 line
HAOT <8 Ma
HAOT 11.0-8.0 Ma
HAOT 13.9-13.1 Ma
Newberry Volcano
0.704
0.706
Medicine Lake Volcano
Modoc Plateau
LATE TERTIARY AND QUATERNARY BASALTS
4-0 Ma
8-4 Ma
Isochron for HAOT initiation

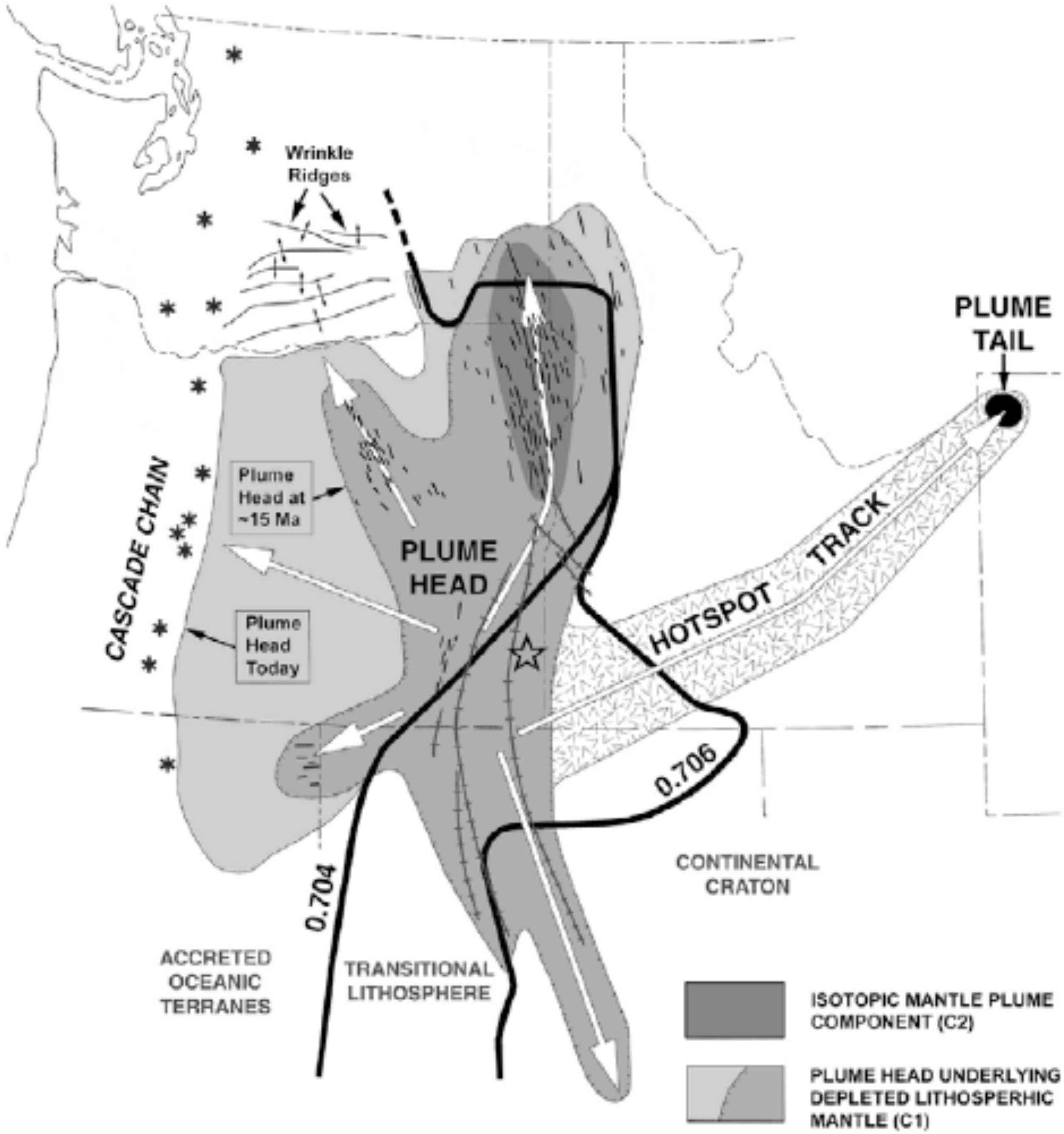

Wrinkle Ridges
PLUME TAIL
CASCADE CHAIN
Plume Head at ~15 Ma
PLUME HEAD
Plume Head Today
HOTSPOT TRACK
0.706
0.704
CONTINENTAL CRATON
ACCRETED OCEANIC TERRANES
TRANSITIONAL LITHOSPHERE
ISOTOPIC MANTLE PLUME COMPONENT (C2)
PLUME HEAD UNDERLYING DEPLETED LITHOSPERHIC MANTLE (C1)

# A plume-triggered delamination origin for the Columbia River Basalt Group

Camp and Hanan 2008

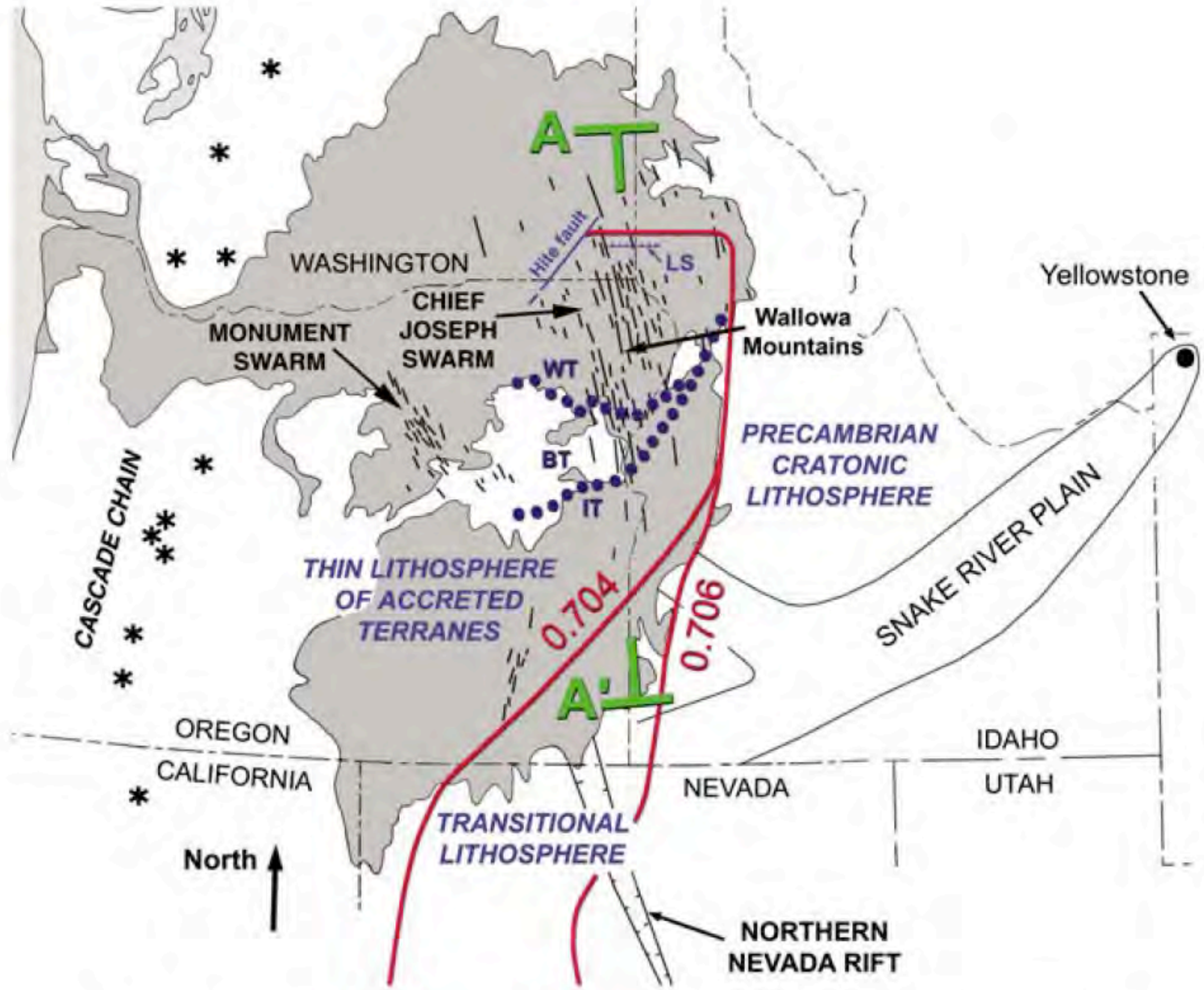


**Figure 1. The Columbia River Flood Basalt Province. Red lines correspond with initial $^{87}Sr/^{86}Sr$ isopleths marking the boundaries between accreted oceanic terranes west of the 0.704 line, and the Precambrian craton east of the 0.706 line (Fleck and Criss, 2004; Pierce et al., 2002). Transitional lithosphere exists between the 0.704 and 0.706 lines. Dotted lines separate the Izee (IT), Baker (BT), and Wallowa (WT) terranes. LS is the "Lewiston structure." A–A' corresponds with the cross-section diagrams in Figure 7 and the topographic profile in Figure 8B.**

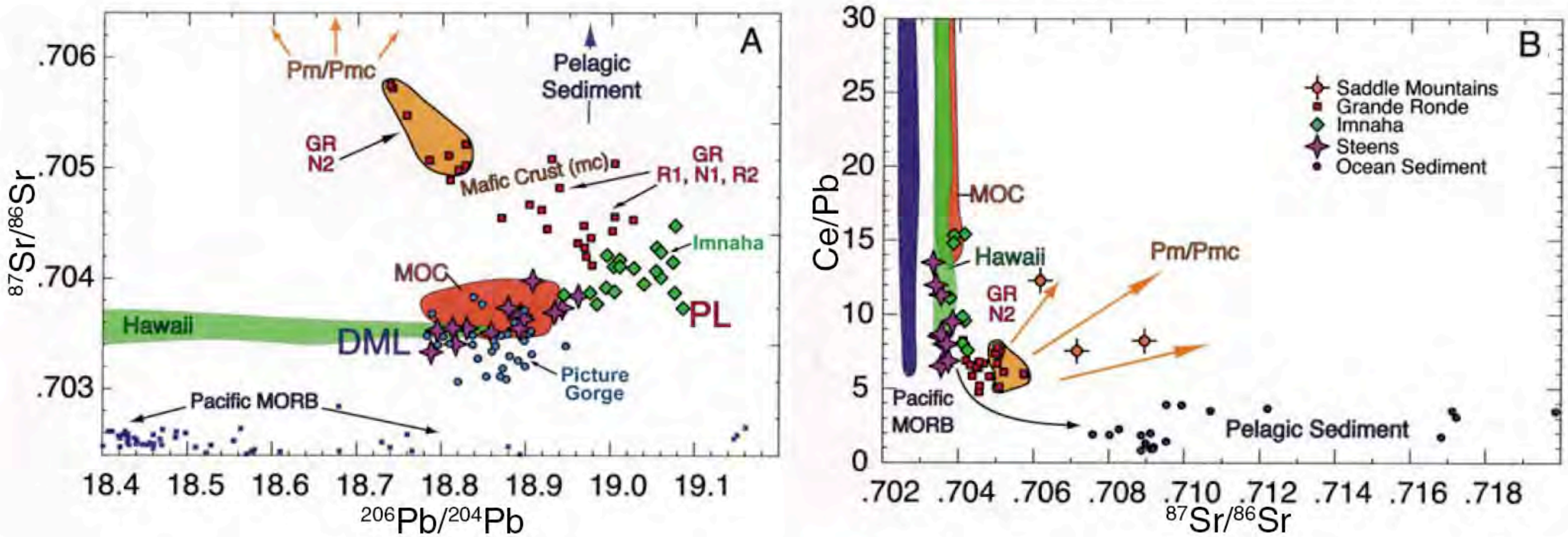


**Figure 2.** (A) $^{87}$Sr/$^{86}$Sr versus $^{206}$Pb/$^{204}$Pb diagram of analyses from the main eruptive phase of the Columbia River Basalt Group. Data are from a variety of sources (Carlson, 1984; Carlson et al., 1981; Hooper and Hawkesworth, 1993; Brandon et al., 1993), with new analyses presented here on Steens Basalt (Table 1). Depleted upper mantle *(DML,* the C1 component of Carlson, 1984), plume mantle *(PL,* the C2 component of Carlson, 1984), mafic crust of Paleozoic-to-Mesozoic age *(mc)*, mafic crust of Precambrian age *(Pmc)*, and Precambrian mantle lithosphere *(Pm)* are presumed source components for the Columbia River Basalt Group. Note that the Grande Ronde lavas deviate from the mantle array toward older lithospheric components *(mc, Pmc, Pm)* and/or oceanic sediment components. The Grande Ronde N2 lavas have high $^{87}$Sr/$^{86}$Sr and distinctly lower $^{206}$Pb/$^{204}$Pb relative to the stratigraphically lower R1, N1, and R2 lavas, consistent with the input of a cratonic component to the younger N2 lava source. Younger lavas from the Wanapum and Saddle Mountains Formations are not shown, but are generally more isotopically evolved (Saddle Mountains lavas all have $^{87}$Sr/$^{86}$Sr >0.706), consistent with components from the enriched Archean lithosphere (Carlson, 1984; Hooper and Hawkesworth, 1993). Pelagic ocean sediment has $^{87}$Sr/$^{86}$Sr >0.706 and plots off the figure at this scale. Pacific mid-ocean ridge basalt (MORB) represents the East Pacific Rise north of 23°S (Hanan and Graham, 1996; Pet DB). Also shown is the field for Pacific Mesozoic Oceanic crust (MOC; Shervais et al., 2005) and Hawaiian Island shield tholeiites (GeoRoc). Note that the Hawaii intra-plate plume basalts overlap with the Steens and Picture Gorge Basalts, but not with the Imnaha or Grande Ronde Basalts. (B) $^{87}$Sr/$^{86}$Sr versus Ce/Pb with the same data set as (A), but with Ce/Pb data for Steens Basalt from J. Wolff (2008, personal commun.). Ce/Pb is a sensitive indicator of crustal components in the mantle. The Pacific MORB, Hawaii shield basalts, and Pacific Mesozoic Oceanic crust (MOC) all show a wide range in Ce/Pb that suggests pollution of their mantle source by pelagic sediment. Note that Hawaii and the accreted MOC basalts are very similar in $^{87}$Sr/$^{86}$Sr, Ce/Pb, and radiogenic Pb isotopes. This illustrates the difficulty in differentiating between recycled oceanic lithosphere that may be a plume source (e.g., Hawaii) and accreted oceanic lithosphere. The Steens and Picture Gorge Basalts are more similar to the Hawaii plume basalts and MOC than is Imnaha Basalt. We could therefore just as readily tie the Steens and Picture Gorge Basalts to the plume composition. Imnaha Basalt would then represent the plume polluted by the Mesozoic accreted terranes, with some Paleoproterozoic cratonic component. The Grande Ronde is mainly accreted terrane lithosphere and/or crust variably polluted by more of the cratonic component.

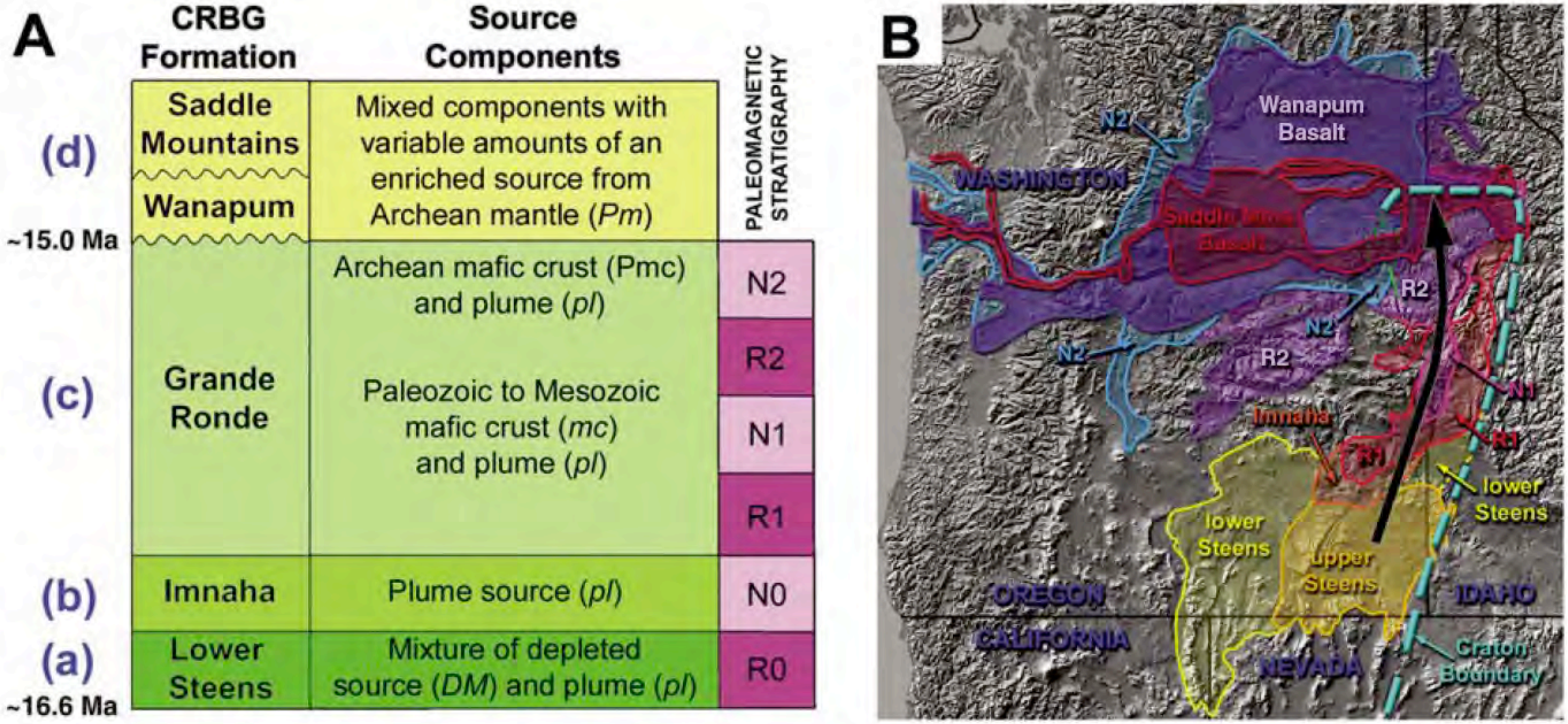


**Figure 5.** Stratigraphy and map distribution of main Columbia River Basalt Group (CRBG) units. (A) Stratigraphy and source components of the Columbia River Basalt Group units that erupted along cross-section A–A' in Figure 1. Letters (a)–(d) correspond with the evolution of each formation as depicted in the cross-sectional diagrams of Figure 7. Paleomagnetic units R0–N2 correspond with sequential reverse and normal paleomagnetic intervals during the main-phase eruptions. The terms lower Steens and upper Steens Basalts are defined in Hooper et al. (2002) and Camp et al. (2003). Imnaha Basalt clearly overlies lower Steens Basalt in the Malheur Gorge of eastern Oregon (Hooper et al., 2002). The stratigraphic relationship between Imnaha Basalt and upper Steens Basalt is poorly constrained, although they may be interbedded with one another south of the Malheur Gorge region (Camp et al., 2003). (B) Map distribution of main Columbia River Basalt Group units. Northward migration of volcanism is evident in the northward offlap of progressively younger units from southeastern Oregon into northeastern Oregon and adjacent Washington State.

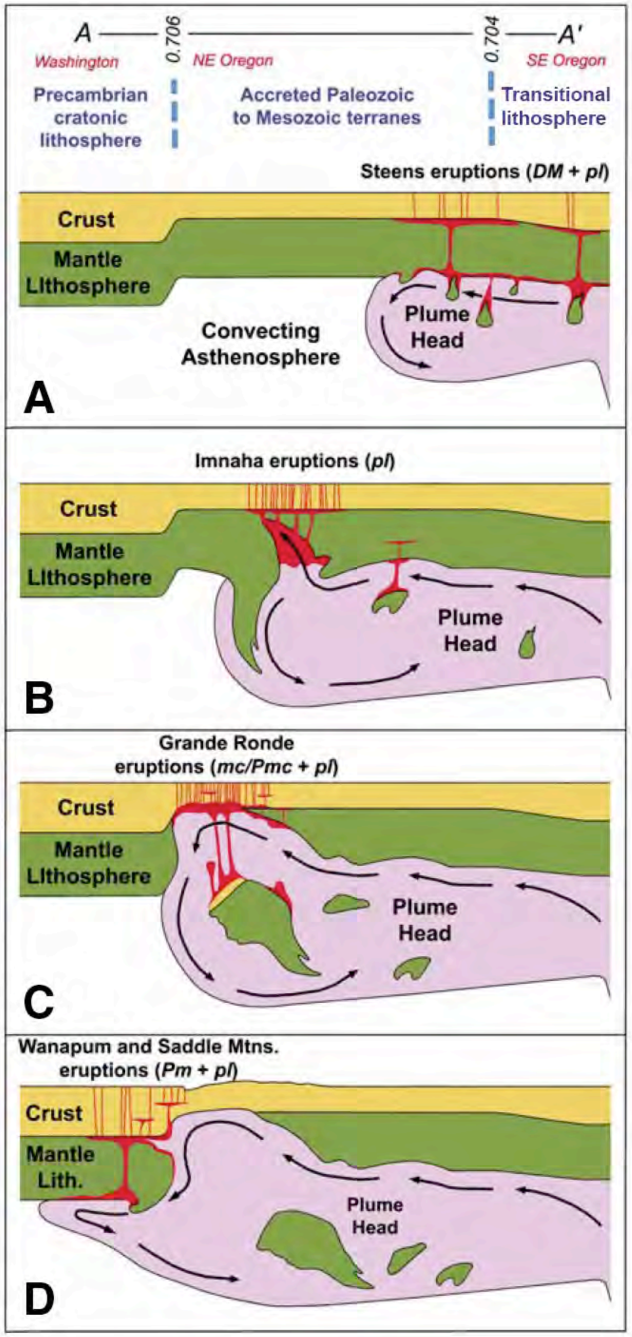


**Figure 7.** Plume-induced delamination model for the Columbia River Basalt Group, based partly on the thermo-mechanical experiments of Burov et al. (2007). Cross-sections (A)–(D) correspond with the age-progressive evolution of the Columbia River Basalt Group stratigraphy (Fig. 5) as the plume head advanced northward along the cross-section A–A' in Figure 1. (A) Plume impingement in southeast Oregon generates drip-like delamination of depleted lithospheric mantle *(DML)* into the hot plume head, as predicted by the model of Burov et al. (2007), thus generating Steens basalt. (B) As the plume spreads to the north, slab-like delamination predicted by the model allows the mobile plume head *(PL)* to rise into the lithospheric void, thus generating more enriched melts of Imnaha Basalt that erupt from incipient fissures in the Chief Joseph dike swarm. (C) The delaminated slab simultaneously descends into the hot plume head. With the plume temperature lying well above the solidus temperature of basalt, mafic lower crust *(mc)* of the delaminated slab undergoes near-wholesale melting to produce the voluminous Grande Ronde succession. (D) As the plume impinges against the cratonic boundary, more isotopically evolved lavas of the Grande Ronde N2 paleomagnetic unit are generated from the melting of Archean lower crust *(Pmc)*, followed by sporadic eruptions of Wanapum and Saddle Mountains Basalts, generating melts with an increasingly greater component of Archean mantle lithosphere *(Pm)*. After the main-phase Columbia River Basalt Group eruptions, mildly alkaline to calc-alkaline lavas and high-alumina olivine tholeiites erupted discontinuously above the plume head in southeastern Oregon, during a time of crustal extension at the northern margin of the Basin and Range province (Hart et al., 1984; Cummings et al., 2000; Brueseke et al., 2007; Hooper et al., 2002, 2007).

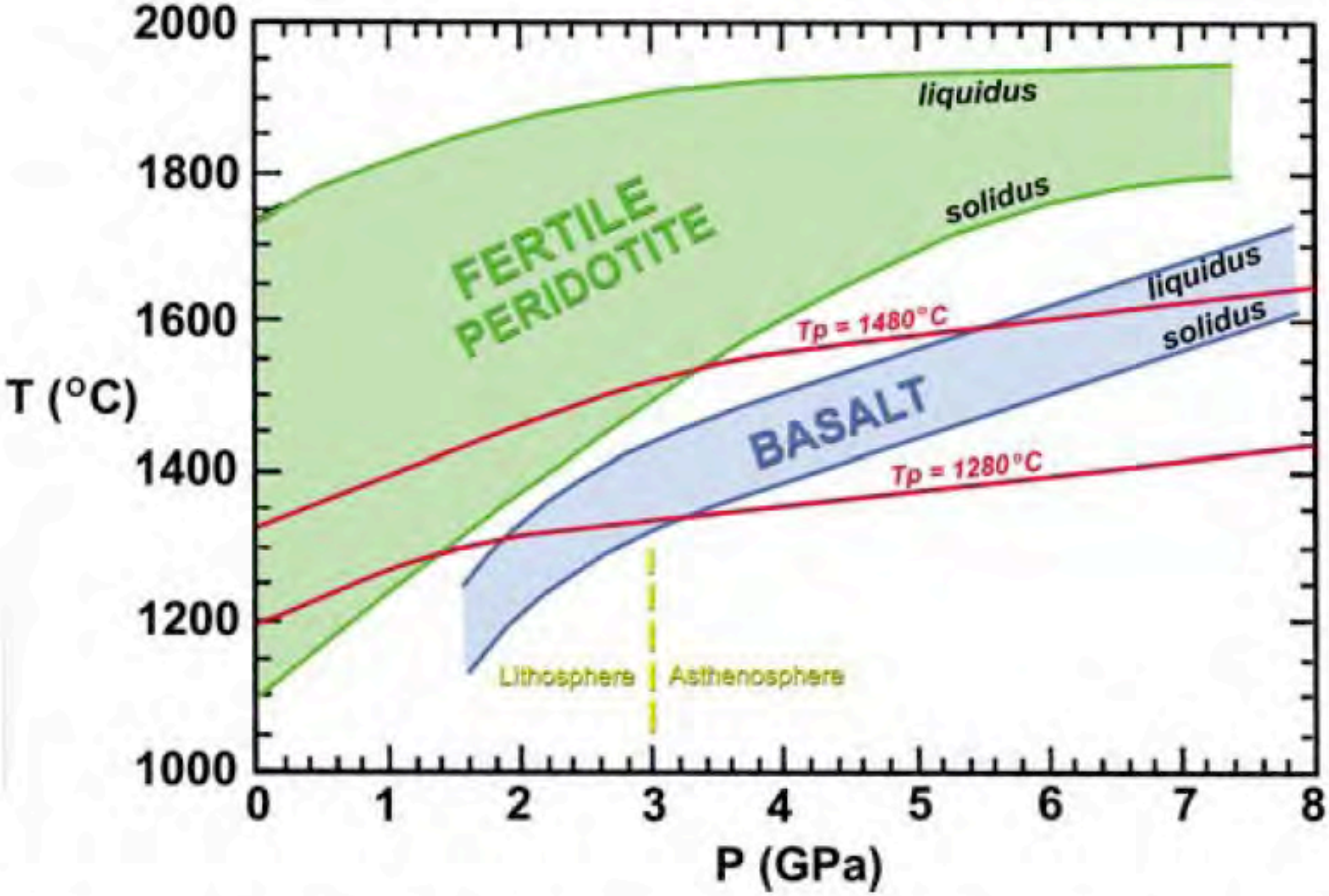


**Figure 6. Solidi and liquidi for average mid-ocean ridge basalt (MORB) (Yasuda et al., 1994) and fertile peridotite (McKenzie and Bickle, 1988). Mantle adiabats for potential temperatures of 1280 °C and 1480 °C from Miller et al. (1991a, 1991b). Modified from Yaxley (2000). A pressure interval of 1.0 GPa is equivalent to ~35 km depth.**

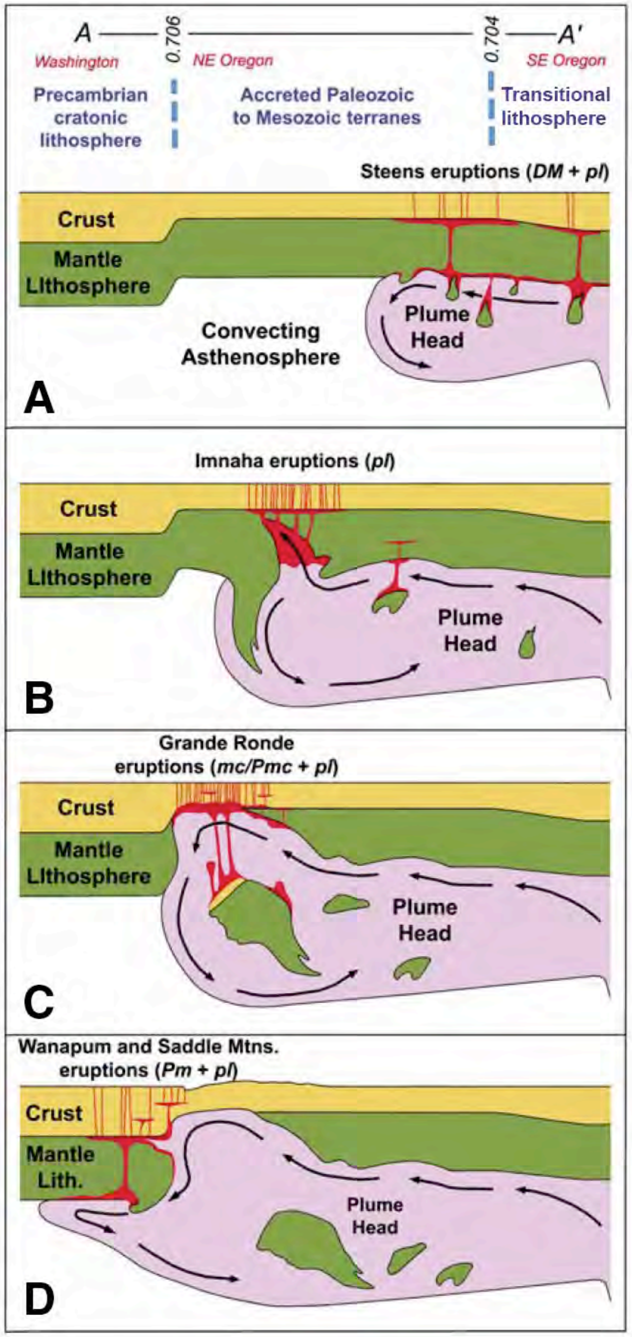


**Figure 7.** Plume-induced delamination model for the Columbia River Basalt Group, based partly on the thermo-mechanical experiments of Burov et al. (2007). Cross-sections (A)–(D) correspond with the age-progressive evolution of the Columbia River Basalt Group stratigraphy (Fig. 5) as the plume head advanced northward along the cross-section A–A' in Figure 1. (A) Plume impingement in southeast Oregon generates drip-like delamination of depleted lithospheric mantle *(DML)* into the hot plume head, as predicted by the model of Burov et al. (2007), thus generating Steens basalt. (B) As the plume spreads to the north, slab-like delamination predicted by the model allows the mobile plume head *(PL)* to rise into the lithospheric void, thus generating more enriched melts of Imnaha Basalt that erupt from incipient fissures in the Chief Joseph dike swarm. (C) The delaminated slab simultaneously descends into the hot plume head. With the plume temperature lying well above the solidus temperature of basalt, mafic lower crust *(mc)* of the delaminated slab undergoes near-wholesale melting to produce the voluminous Grande Ronde succession. (D) As the plume impinges against the cratonic boundary, more isotopically evolved lavas of the Grande Ronde N2 paleomagnetic unit are generated from the melting of Archean lower crust *(Pmc)*, followed by sporadic eruptions of Wanapum and Saddle Mountains Basalts, generating melts with an increasingly greater component of Archean mantle lithosphere *(Pm)*. After the main-phase Columbia River Basalt Group eruptions, mildly alkaline to calc-alkaline lavas and high-alumina olivine tholeiites erupted discontinuously above the plume head in southeastern Oregon, during a time of crustal extension at the northern margin of the Basin and Range province (Hart et al., 1984; Cummings et al., 2000; Brueseke et al., 2007; Hooper et al., 2002, 2007).

Snake River Plain. View to northeast

# Snake River near Caldwell, ID

# Snake River Plain near Caldwell, ID

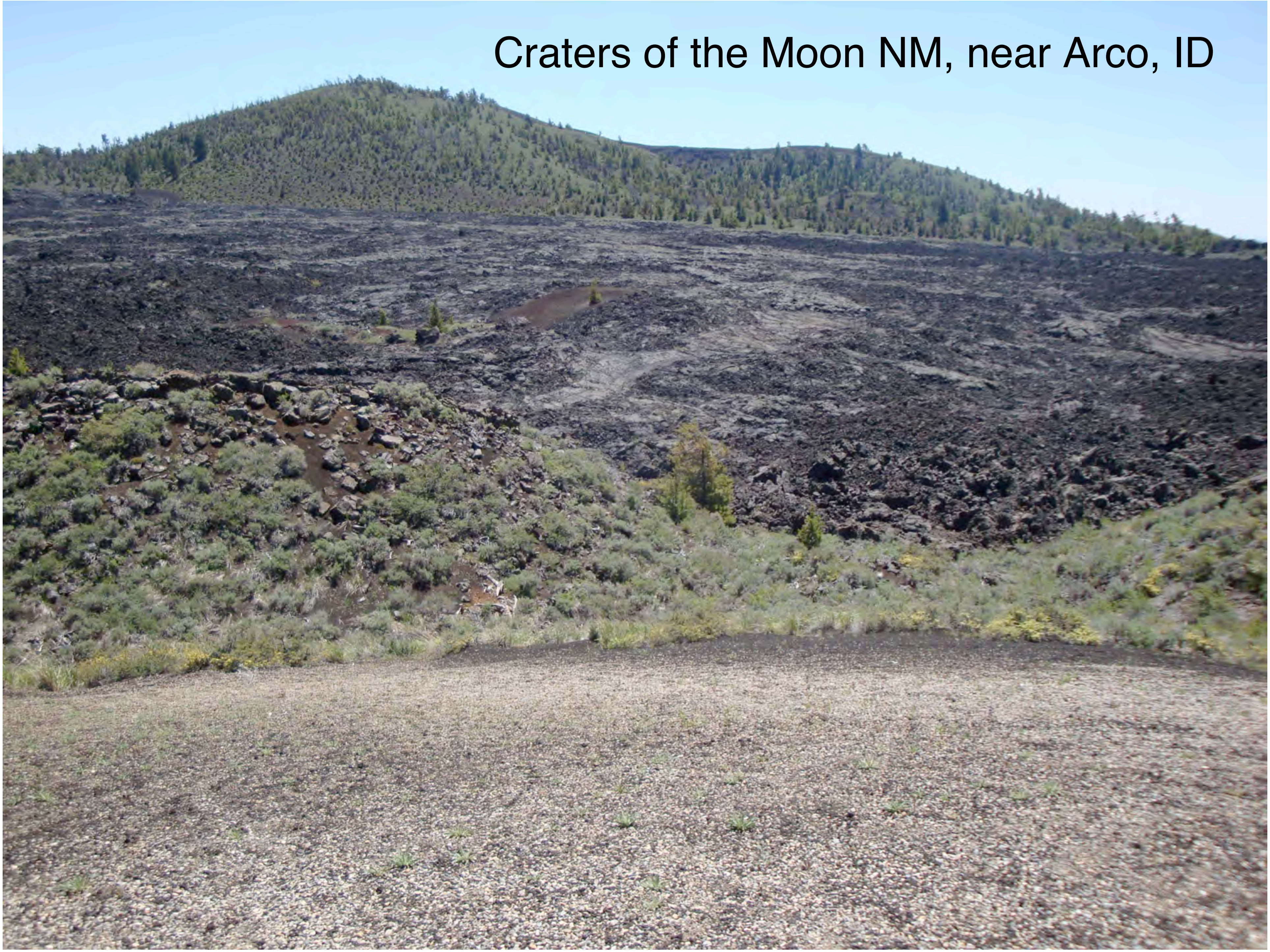
Craters of the Moon NM, near Arco, ID

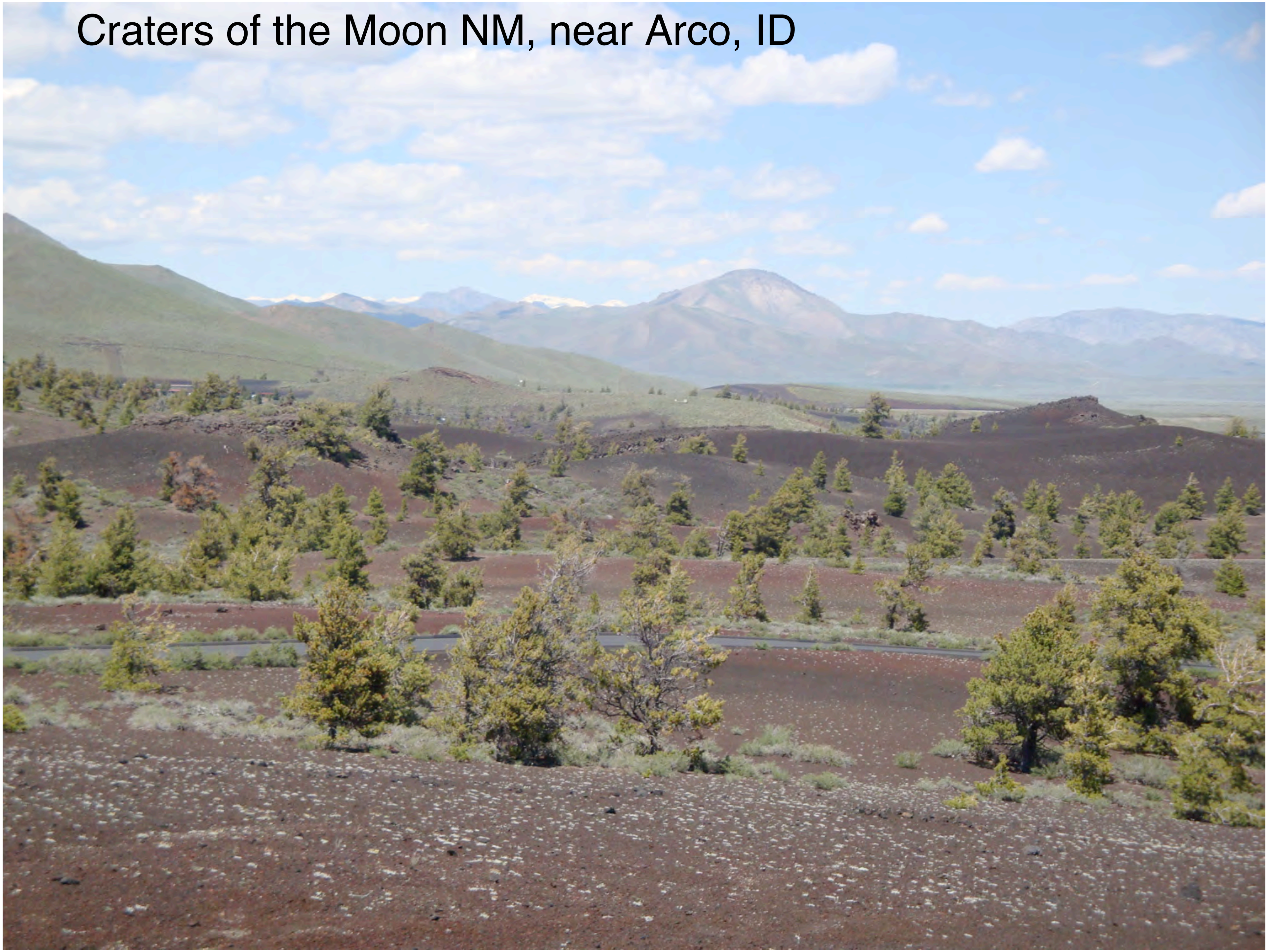
Craters of the Moon NM, near Arco, ID

Craters of the Moon NM, near Arco, ID

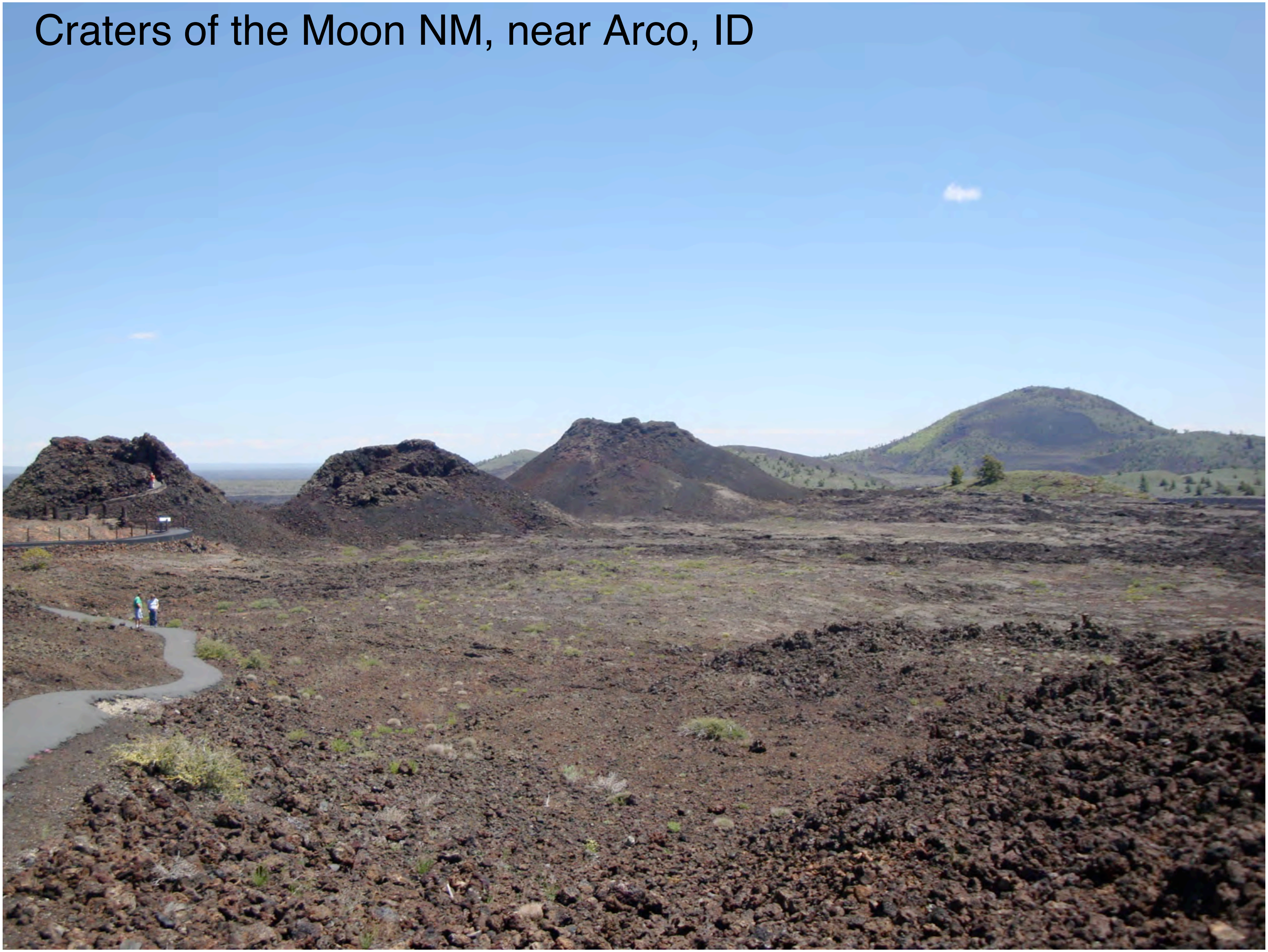

Two of Three Buttes, near Idaho Fall, ID


Old Faithful Geyser, Yellowston NP, WY

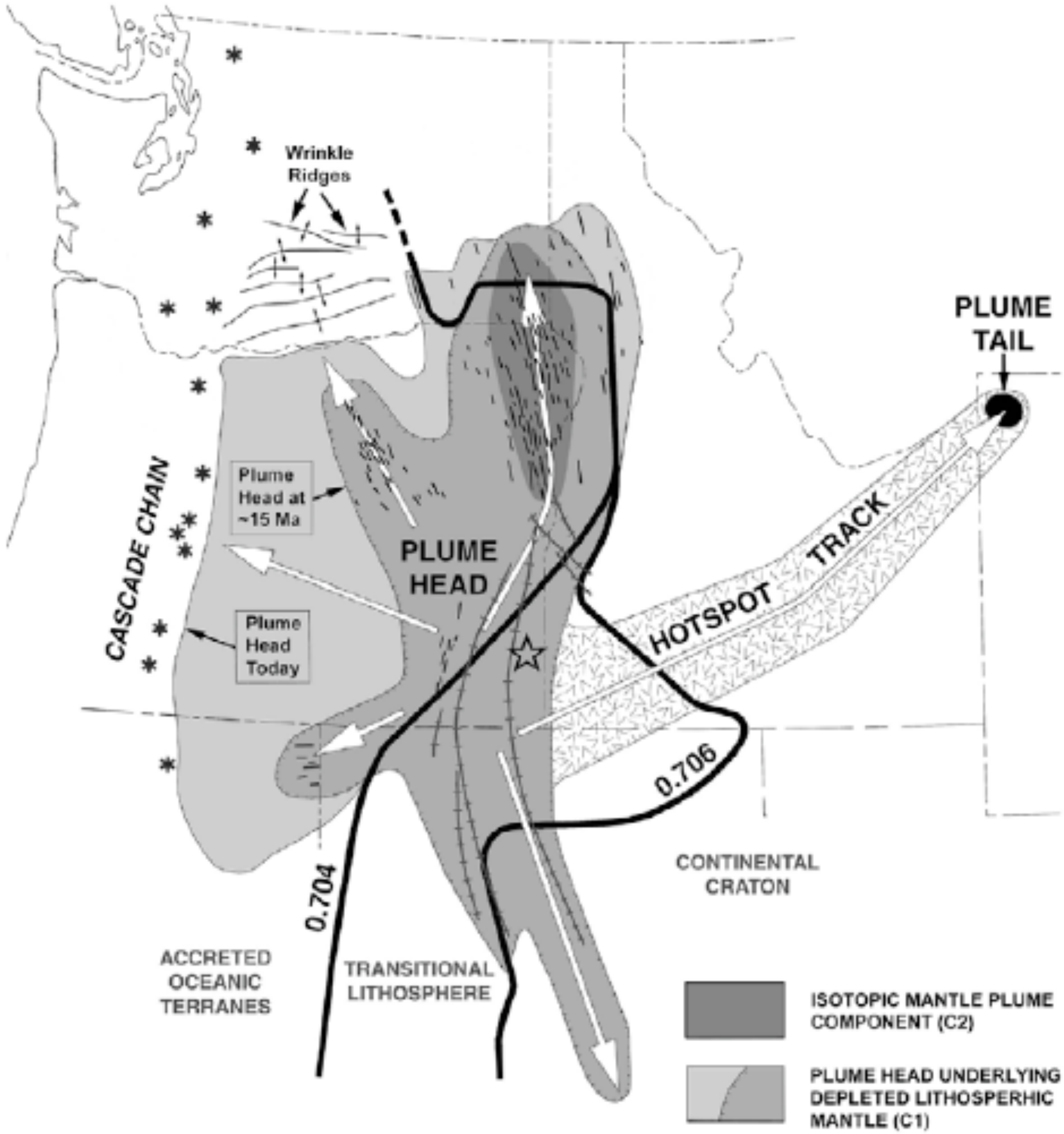
Wrinkle Ridges
PLUME TAIL
CASCADE CHAIN
Plume Head at ~15 Ma
PLUME HEAD
Plume Head Today
HOTSPOT TRACK
0.706
0.704
CONTINENTAL CRATON
ACCRETED OCEANIC TERRANES
TRANSITIONAL LITHOSPHERE
ISOTOPIC MANTLE PLUME COMPONENT (C2)
PLUME HEAD UNDERLYING DEPLETED LITHOSPERHIC MANTLE (C1)

# Upper mantle origin for the Yellowstone hotspot

Christiansen et al 2002

GSA Bulletin pp. 1245-1256.

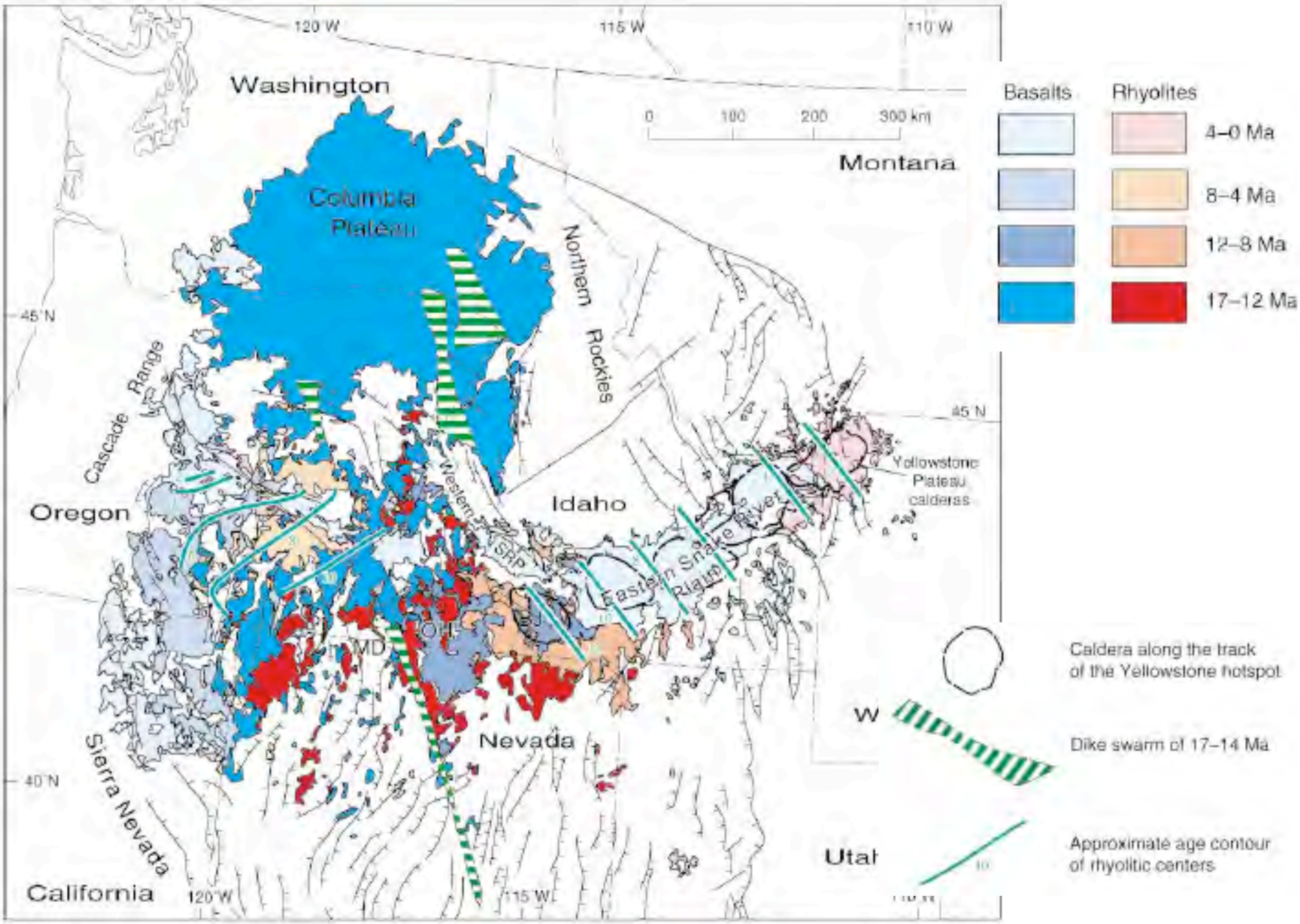

120°W
115°W
110°W
Washington
0
100
200
300 km
Montana
Basalts
Rhyolites
4–0 Ma
8–4 Ma
12–8 Ma
17–12 Ma
Columbia Plateau
Northern Rockies
45°N
Cascade Range
Yellowstone Plateau calderas
Oregon
Western SRP
Idaho
Eastern Snake River Plain
MD
OH
Caldera along the track of the Yellowstone hotspot
W
Dike swarm of 17–14 Ma
Sierra Nevada
Nevada
40°N
Utah
Approximate age contour of rhyolitic centers
California

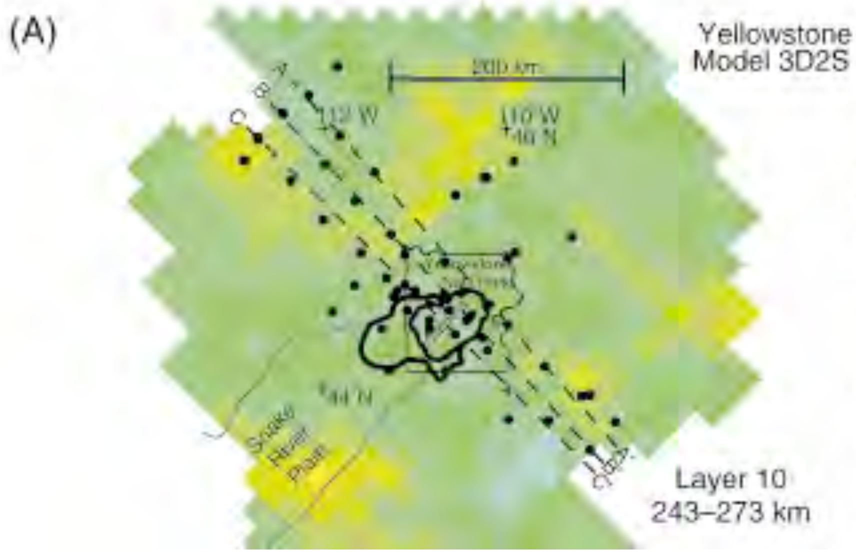


Figure 2. Teleseismic tomographic structure beneath Yellowstone obtained with the techniques of Evans and Achauer (1993) on a subset of the data collected by Iyer et al. (1981). Data were selected for uniform coverage in event back-azimuth and distance, optimizing the ray set. The color scale shown in D applies to all parts of the figure; distance and depth scaling are also constant; small circles in some of the blocks indicate that the velocity anomalies exceed the range of the color scale. (A) Dots are the stations used; the boundary of Yellowstone National Park and the edges of the eastern Snake River Plain are shown; lines of cross section shown in B, C, and D are indicated. Colors indicate wave-speed variations in the layer in the depth interval 243–273 km, where a deep plume-like structure would be imaged if one exists. Irregularly shaped, closed rings outline calderas of the Yellowstone Plateau volcanic field (Christiansen, 2001).

# Tomographic Images showing NO deep mantle hot spot

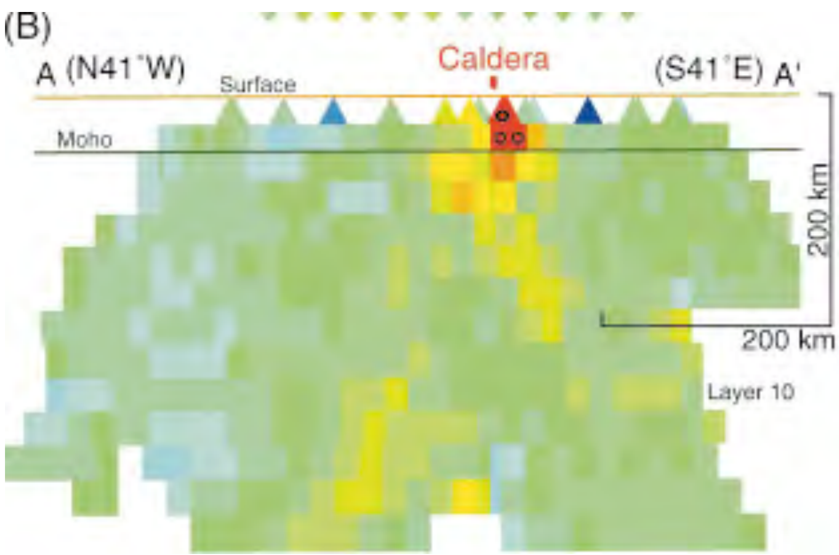


(B) Cross section through the model at the northeast edge of the caldera, presumed by some investigators to be the center of the hotspot. (C) and (D)

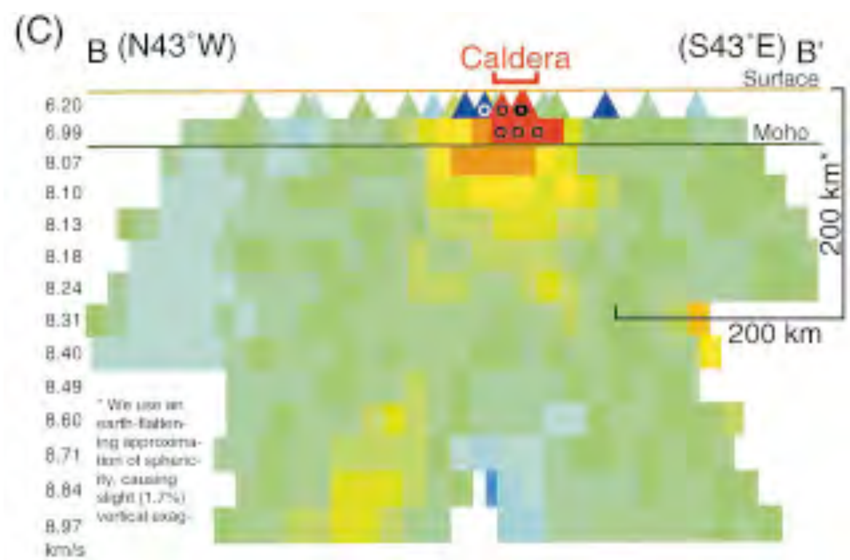


tigators to be the center of the hotspot. (C) and (D) Cross sections farther southwest through the caldera.

Field Trip
Check the Weather Forecast!
Bring Appropriate Clothing!
Sneakers are OK
Boots are OK
Sandals and Flip-Flops may be problematic!
Sunscreen
Sunglasses
NOTEBOOK AND PEN/PENCIL
RULER
CAMERA
(HAND LENDS
WATER
LUNCH
SNACKS